A 10,000-year lake-sediment based reconstruction of precipitation isotope values in the Canadian Rocky Mountains and implications for past changes in North American hydroclimate

A thesis
SUBMITTED TO THE FACULTY OF THE
UNIVERSITY OF MINNESOTA
BY

Zachary C Wagner

IN PARTIAL FULFILLMENT OF THE REQUIREMENTS

FOR THE DEGREE OF

MASTER OF SCIENCE

Dr. Byron Steinman

January 2019

Acknowledgements

I owe many people thanks for helping me get to this point. First, my advisor Byron Steinman, for guiding me on this project and giving me such great academic opportunities. It was amazing to be a part of coring trips to Isle Royale, Manitoba, the Canadian Rockies and Pacific Northwest. I was also fortunate to have opportunities to work with other paleolimnologists. I want to thank Mark Abbott and Nathan Stansell for opening their labs to me and helping me obtain important data. Also, thank you to lab and research staff at UMD, especially Julie Halbur, Aaron Lingwall, and Tsutomu "Shimo" Shimotori for providing assistance in data collection.

Thank you to my fellow students in the Earth and Environmental Sciences department and at the Large Lakes Observatory. I'd especially like to thank Kat Vall and Chris Shea, the grad students also working in the Steinman lab. I was fortunate to have such a good team that helped each other and made work fun. I have so many good memories from our field and research trips. I also had undergraduate students Bryan Crum, Hanna Leapaldt, and Jenny Sherren working with me, and I thank them for their help with keeping my sediment analysis moving. Finally, I want to thank my wife Erica for supporting me through this entire process. You kept me going on this project the whole time and did so much to help me.

Funding for this project was provided by the National Science Foundation.

Abstract

Hydroclimate change in the Canadian Rocky Mountains is an important area of research, as demand for water resources in the Great Plains has been continuously increasing in recent years. The population of Alberta has one of the fastest growth rates in Canada, and cities like Calgary and Edmonton are dependent on surface and groundwater resources that originate from precipitation in the mountains. Recent increases in petroleum exploration have also amplified demands for water, along with the growing water requirements of industrial agriculture. The application of sound water resource management policies is essential, and historical records span only ~200 years, a time frame too short to capture the full range of climate variability. The development of paleoclimate proxy records from the Rocky Mountains is therefore necessary to attain a thorough perspective on potential changes in climate. Such data can, for example, inform water resource managers of possible shifts in precipitation seasonality and drought/pluvial events on timescales of decades to millennia. To this end, we present a 10,000-year oxygen isotope record as a proxy for precipitation seasonality linked to the Pacific North American pattern (PNA) which adds to a growing body of research in a region of high spatial complexity of hydroclimate.

Shark Lake in Alberta, CA (50.8412°N, 115.3990°W; 1857 m above sea level) is a hydrologically open basin lake in the Canadian Rocky Mountains with one large outlet and numerous small inlets and groundwater springs. Winter precipitation is more depleted in the heavier ^{18}O isotope relative to summer precipitation due to equilibrium fractionation from rain-out and phase changes. $\delta^{18}O$ and δD values of Shark Lake water samples (collected during the summer) range from -18.9 to -20.0 ‰ and -141 to -150 ‰, respectively. The annual weighted average precipitation isotope ratios are -16.6 and -126 ‰ for oxygen and hydrogen, respectively. This indicates that Shark Lake principally receives water inputs from runoff or shallow groundwater that originated as precipitation during the cold season. We collected 1 m and 1.5 m long sediment cores using a modified Livingstone corer and used loss-on-ignition (LOI), x-ray diffraction (XRD), x-ray fluorescence (XRF) analyses to destermine sediment texture and composition. The sediment was dated using ^{14}C from terrestrial plant fossils, as well as ^{210}Pb and ^{137}Cs for the surface sediment. We analyzed the isotopic composition ($\delta^{18}O$) of authigenic

carbonate sediment from Shark Lake using mass spectrometry and applied these results as a proxy for precipitation seasonality.

Lake water oxygen isotope ratios are captured by authigenic carbonates, which form during the spring and summer in response to pH changes associated with primary production. These carbonate minerals (calcite) precipitate in isotopic equilibrium and are deposited on the lakebed where they are preserved. The Shark Lake $\delta^{18}O$ record demonstrates a transition from lower to higher average $\delta^{18}O$ values from the middle to the late-Holocene at around 4500 yr BP. This is consistent with previous findings of changes in PNA-like atmospheric patterns during the middle Holocene, when a gradual shift from a more negative to a more positive mean state phase of the PNA occurred. This produced enhanced zonal atmospheric circulation in the Pacific Basin that led to a reduction in winter precipitation in northwestern North America and drier conditions in the southwestern part of the continent in the late Holocene relative to the middle Holocene.

The Shark Lake $\delta^{18}O$ record has a positive, significant correlation with other similar records from the Pacific Northwest, specifically those from Lime Lake (WA) and the OCNM (OR) speleothem, and has a negative, significant correlation with records from the southern Rocky Mountains and eastern North America, namely those from Bison Lake (CO), Cheeseman Lake (NL), Grinnell Lake (NJ), and the Buckeye Creek Cave speleothems (WV). Decadally resolved records are useful for tracking changes in PNA state and its interaction with other related climate oscillations such as the El Niño Southern Oscillation (ENSO) and the associated Pacific Decadal Oscillation (PDO). Open-basin lake records can also be combined with hydrologically closed-basin lake records to reconstruct pluvial and drought periods over the Holocene. The Shark Lake record increases the spatial resolution of mid- to late Holocene hydroclimate climate data in the Rocky Mountains and provides a baseline for natural variability in precipitation seasonality in a hydrologically important region.

Table of Contents

List of Tables

Supplemental Data Tables

List of Figures

1. Introduction

Societal dependence on water resources drives the need to better understand changes in precipitation timing, amount, and phase on timescales longer than the instrumental record in order to account for the full range of climate variability when establishing water resource policies. The Canadian Rocky Mountains are an important source of water for over four million people in Alberta, and that population has been steadily growing by about 10% every five years since the year 2000 (Sauchyn et al. 2015). Agriculture and tar sands petroleum extraction, which has recently expanded, are both heavy users of surface and groundwater from the Rockies. In 2015, 18.3% of the Alberta gross domestic product (GDP) was from oil and gas extraction, amounting to about 61 billion United States dollars (Alberta Treasury Board). In addition to being an iconic part of Alberta's image, the lakes and rivers of the Rockies provide opportunities for tourism and recreation, which made up 4.8% of Alberta's GDP in 2015. Much of the water resources used in the Great Plains either comes from snow/glacier melt runoff or shallow groundwater, and both sources depend on alpine snowpack in the Rockies for recharge (Sauchyn et al. 2003; Larson et al. 2011). Ice fields and glaciers have been shrinking in the Rocky Mountains since the Little Ice Age expansion in the late 1700s and mid-1800s (Smith et al. 1995; Luckman 2000). While mountain water sources are a major concern, changing mountain climate is an additional issue for conservation and forestry due to and increased fire danger from droughts (Fleming and Sauchyn 2013; Sauchyn et al. 2015; Marshall et al. 2011). The main objective of this research is to produce records of hydroclimate change in the Canadian Rocky mountains that will provide Holocene context for understanding changes in seasonal water availability. These records will be compared to similar datasets from elsewhere in North America, in order to explore the possibility of coherent, continent scale shifts in climate from the middle through late Holocene and teleconnections to Pacific ocean-atmosphere circulation dynamics.

Regional studies in the Rocky Mountains and Pacific Northwest show that large-scale climate variations such as millennial-scale glacial and inter-glacial cycles result from changes in solar output and orbital cycles (Asmerom et al. 2007; Ersek et al. 2012).

Solar forcing can also affect Pacific sea surface temperatures (SST), which in turn change atmospheric circulation patterns that affect terrestrial climate. Several climate studies focused on the Rocky Mountains have investigated interannual to decadal variability of the Pacific North American pattern (PNA) (Liu et al. 2014; Sauchyn et al. 2015), which is characterized by atmospheric pressure anomalies over North America (Yu and Zwiers 2007; Bird et al. 2017). The PNA is influenced by oceanic oscillations like the Pacific Decadal Oscillation (PDO), which is closely linked the El Niño Southern Oscillation (ENSO), and atmospheric modes such the Northern Annular Mode/Arctic Oscillation (NAM/AO) (Barron and Anderson 2011; Anderson 2011; Steinman et al. 2016). These internal climate modes/oscillations are the main controls on hydroclimate dynamics in the Rocky Mountains, with the PNA playing a particularly important role as the main control on atmospheric circulation over North America (Anderson et al. 2016; Liu et al. 2014; Sauchyn et al. 2015; Steinman et al. 2016; Mantua and Hare 2002; Sung et al. 2014). Investigating how changes in the PNA strength, phase and teleconnections to ocean dynamics over the Holocene were controlled by external forcing mechanisms (such orbital forcing and solar output) is important for understanding North American climate variability on long time scales. The statistical comparison of hydroclimate records produced as part of this research provides additional evidence for testing the hypothesis that changes in atmospheric circulation dynamics with a PNA-like signature occurred coherently across North America during the middle Holocene.

High resolution paleoclimate data from the Canadian Rocky Mountains is largely from dendroclimatology studies and historical records; however most of these datasets are not continuous and extend to no more than 1,000 years before present (BP), which is too short a time period to capture century timescale climate variability. Paleoenvironmental records from lake sediment, however, have the potential to provide information that extends well beyond the last millennium, with potentially high temporal resolution, and in the Rocky Mountains can reach as far back as the time of deglaciation in the early Holocene. Lake sediment cores have been used to reconstruct land cover, glacial history, and lake productivity using pollen, sediment texture (e.g. grain size) and sediment composition in various places throughout the world (Beierle et al. 2003; Briffa et al. 1992; Shuman et al. 2018). These records tend to be low resolution (century scale or

longer) with limited age control (i.e. high age model uncertainty) and therefore do not capture decadal scale climate variability. Pollen has been used to reconstruct climate using vegetation assemblages and their correlation to either temperature or precipitation. Pollen records are especially helpful for investigating long timescale climate change such as transitions out of glaciation, since they record biologic succession (Davis and Botkin 1985). Lake/catchment environmental changes can be indicated by changes in sediment texture as well. For example, the presence of organic rich sediment can indicate higher lacustrine productivity, which can occur from allogenic nutrients like nitrogen and phosphorus. Organic sediments are often characterized using carbon to nitrogen ratio (C:N) analysis or other organic geochemistry methods to determine the relative amounts of terrestrial versus aquatic organic matter. Organic layers can also be analyzed to indicate water depths on the basis of the presence or absence of littoral plant remains. Clastic material grain size and composition can inform sediment provenance and the depositional energy of the lake floor (Beierle et al. 2003; Rasmussen and Rowan 1997), in that lake depth can be reconstructed from grain size as, for example, sand takes more wave energy to move compared to clay or silt. However, sediment texture is occasionally difficult to interpret; larger grain sizes can result from either increased precipitation (wetter conditions and more clastic movement from the catchment) or lake level regression (drier conditions) and thus a transition toward a near shore depositional setting. Paleolimnological data from lake sediment lithology and pollen are perhaps most useful for putting proxies with a potentially higher temporal resolution in context, in addition to providing insight on past changes lacustrine paleoenvironments (Anderson et al. 2015). Other proxies from in-lake sources like aquatic fossils can inform on lake chemistry like oxygenation or trophic state. Terrestrial data can be also found in multiproxy studies, such as charcoal from forest fires. A multi-proxy approach in which various proxies are applied, and wherein each proxy targets a different component of the larger system, is the best approach to producing a comprehensive reconstruction of past changes in lake/catchment environmental conditions.

Analysis of the oxygen-18 isotope ratios ($\delta^{18}O$) of authigenic carbonate minerals in lake sediment can provide information about changes in catchment specific hydrologic balance and/or the isotopic composition of precipitation, depending on the hydrologic characteristics of the lake (Steinman et al. 2010). Authigenic carbonates forming in isotopic equilibrium in the water column capture the water isotope ratio at the time of mineral formation, with an equilibrium fractionation that is controlled by water temperature (Kim and O'Neil 1997; Kim et al. 2007). Lake water isotopes are controlled by lake water hydrologic balance. Closed-basin lakes, which are strongly influenced by the balance between precipitation and evaporation will contain water more enriched in oxygen-18 due to equilibrium and kinetic fractionation processes that occur during evaporation from the lake surface. Open-basin lakes that are not influenced by evaporation (or at least minimally so) will contain water that reflects the isotopic composition of inflowing meteoric water derived from seasonal precipitation. Precipitation isotope values change throughout the year due to changes in the extent of equilibrium fractionation during water phase changes associated with Rayleigh fractionation; summer $\delta^{18}O$ and δD values tend to be enriched in oxygen-18 compared to winter isotope values (Gat 1996). Both long and short timescale ocean-atmosphere circulation variability can cause changes in seasonal precipitation balance which can affect the isotopic composition of meteoric water and thus change lake water isotope values (Rozanski et al. 1992; Steinman et al. 2016; Bird et al. 2017). Catchment hydrology changes related to lake level such as lake overflow or disconnection from inputs can also change lake hydrologic and isotope balance. Changes in oxygen isotope ratios in lacustrine carbonate sediment therefore can be used to reconstruct multi-annual averaged variations in water isotope values which reflect past changes in either catchment scale hydrology and/or regional scale changes in precipitation isotope values. Open basin lake records can be combined with closed basin lake records to reconstruct regional pluvial and drought periods (Steinman et al. 2016).

The objective of this research is to produce a high-resolution record of hydroclimate principally through oxygen isotope analysis of authigenic carbonates in sediment from Shark Lake, southeastern Alberta, Canada (Figure 1). Shark Lake is positioned on carbonate bedrock in relatively undeveloped mountainous terrain,

experiences carbonate mineral 'whiting' events (as evidenced by aerial photographs) and the has an open-basin hydrologic configuration, which offers the potential to reconstruct the isotopic composition of inflowing meteoric water (derived from precipitation on the lake and catchment) and thereby provide insight on large-scale atmospheric circulation patterns. In addition, the Shark Lake record can potentially provide a baseline for oxygen isotope values in meteoric water inputs to closed-basin lakes in the region that will form the basis of subsequent research on local catchment hydrologic balance during the Holocene. Previous research in the Pacific Northwest supports the use of oxygen isotope analysis of authigenic carbonate lake sediments from open- and closed-basin lakes as an effective proxy for reconstructing precipitation isotope values, hydroclimate seasonality, and precipitation amounts (Anderson 2011; Steinman et al. 2016; Steinman et al. 2010).

The general questions that motivate this research along with accompanying specific questions are:

1) Can changes in oxygen isotope values in precipitation be reconstructed using isotope analyses of lacustrine carbonate sediment from open-basin lakes in southeastern Alberta?
    a. Is Shark Lake, Alberta, an open-basin lake with water isotope values consistent with local meteoric water?
    b. Is the carbonate sediment in Shark Lake primarily authigenic and are the oxygen isotope values of the sediment predominantly controlled by changes in meteoric water (e.g. precipitation) isotope values?
    c. What is the extent to which changes in precipitation isotope values have influenced closed-basin lake oxygen isotope records of drought/pluvial events in the southern Canadian Rockies?
2) How have precipitation isotope values varied over the Holocene in the Pacific Northwest, and what are the implications for synoptic scale hydroclimate processes?
    a. Are records of changes in precipitation isotope variability from the southern Canadian Rockies consistent with other, similar records from western North America?

b. Do records of changes in precipitation isotope variability from the southern Canadian Rockies support hypotheses regarding PNA driven atmospheric circulation changes during the Holocene?

We hypothesize:

1) The isotopic composition of carbonate in sediment from open-basin lakes in settings similar to Shark Lake are controlled principally by cold season precipitation isotope values.
    a. Shark Lake is an open-basin lake due to rapid throughflow (e.g. large, active outflows and inflows) and a short residence time, with water isotope values consistent with local meteoric water inputs.
    b. Carbonate sediment is likely authigenic, forming in whiting events that occur during the warm season (spring and/or summer). The carbonate sediment isotope record is therefore reflective of precipitation isotope values since lake water isotope ratios are preserved by authigenic carbonate sediment.
2) Precipitation isotope values have changed over the Holocene, in part reflecting regional climate variations such as droughts and pluvial periods, and in part due to synoptic scale Pacific ocean-atmosphere processes.
    a. Precipitation isotope values from Shark Lake will exhibit trends similar to climate records from the Northern Rockies and elsewhere in the Pacific Northwest due to coherent regional responses associated with large-scale atmospheric circulation changes.
    b. Holocene records of changes in precipitation isotope values from North America will be consistent with the findings of Liu et al. (2014) and demonstrate more positive PNA phase-like conditions during the late Holocene and more negative PNA phase-like conditions during the mid-Holocene.

2. Study Site

Shark Lake (50.8412°N, 115.3990°W; 1,857 m above sea level) is located in Peter Lougheed Provincial Park in the Spray Lakes valley of Alberta, Canada, within the front range of the Canadian Rocky Mountains, a region commonly referred to as Kananaskis Country. The lake has a surface area of ~ 27,000 m^2 and a maximum depth of ~4.3 m. The lake is also known colloquially as Marushka Lake. Precipitation falling on the Shark Lake catchment drains eastward into the Spray Lakes Reservoir and then into the Bow River, which flows to the plains near Calgary, Alberta, and then into the South Saskatchewan River, Lake Winnipeg and ultimately, Hudson Bay. The Bow and Saskatchewan Rivers are important water resources for agriculture and industry across the plains regions (Sauchyn et al. 2015). The Bow River is also the main municipal water source for Calgary, Alberta.

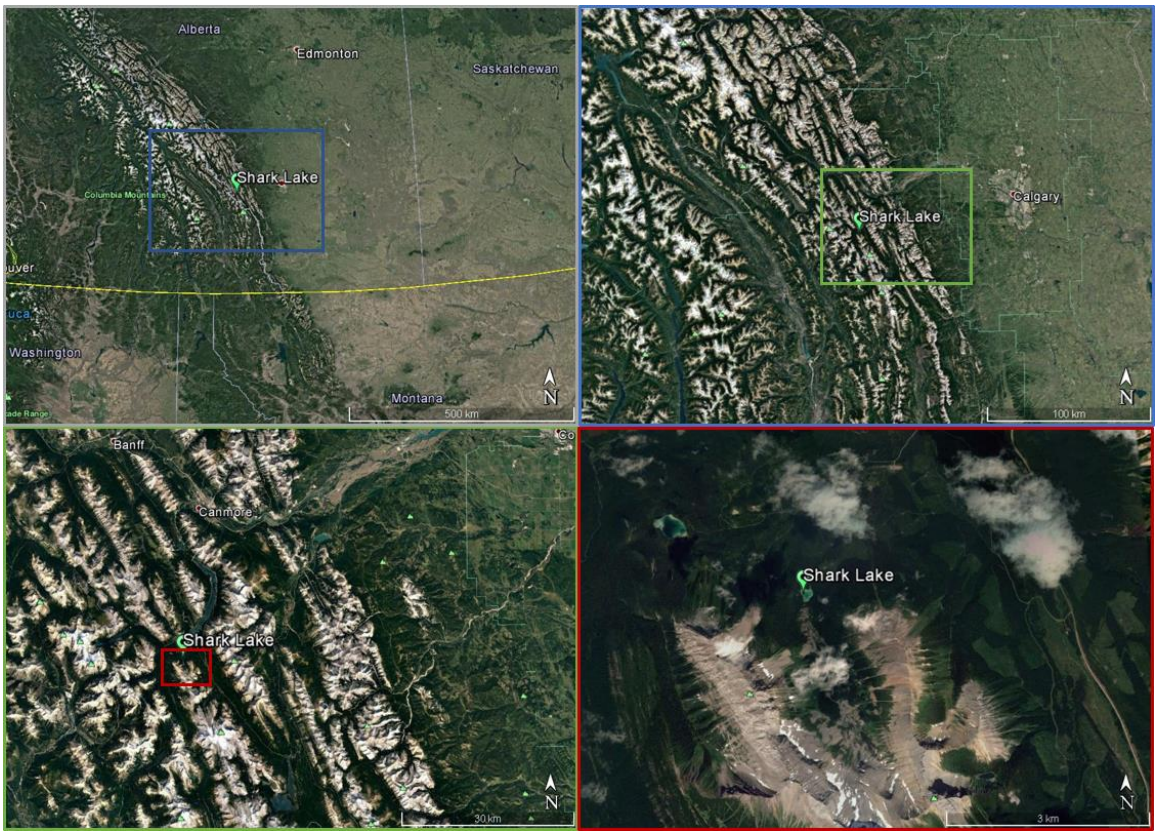

Figure 1 – Lake Location
Shark Lake is located in the eastern range of the Canadian Rocky Mountains, west of Calgary and south of Canmore.

Shark Lake is an open-basin lake with one major outflow, several small inflows and visible groundwater seeps. The basin is characterized by a shallow shelf, which slopes steeply to a deeper, flat bottom. The inflows are focused near the southern most side of the lake where they emerge and cascade through a boulder field. Outflow occurs through a somewhat incised shallow shelf on the northeast side of the lake. Groundwater seeps occur mainly along the bottom of the shelf slope. Dark mats of microbes and organic matter occur near the groundwater seeps.

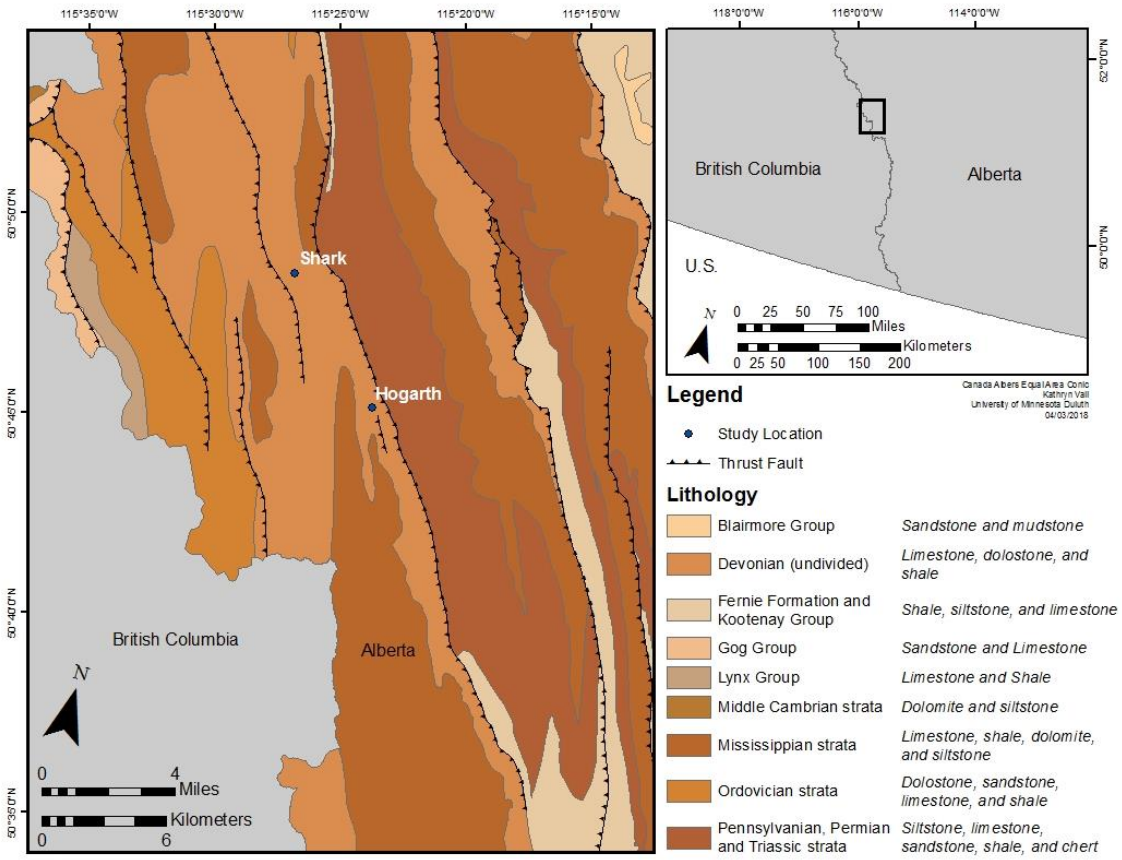

Figure 2 – Bedrock geology
Layers of sedimentary rock are segmented and tilted on fault lines. Shark Lake and its catchment are underlain by Devonian limestone, dolostone, and shale.

Shark Lake is located in a mountain glacial valley depression. The catchment bedrock geology is predominantly Paleozoic carbonate rock and Mesozoic clastic carbonate rocks, including siltstones and mudstones (Sauchynet al. 1998)(Figure 2). The surface deposits are generally thin layers of glacial sediment and organic loam; the exception being scree fields near steep slopes and end moraines. Continental glaciers

associated with the Late Wisconsinin phase receded between 11,000 to 10,000 years before present with the retreat of the Canmore and Crowfoot advances, although alpine glaciers remained well into the Holocene in high elevation cirques in the central and southern mountains of the western cordillera, and some are still present (MacDonald 1989; Bobrowsky and Rutter 1992; Leonard and Reasoner 1999; Evans et al. 1999; Dyke 2004; Osborn and Gerloff 1997; Beierle et al. 2003). The Shark Lake catchment has a north-northwest aspect, and deglaciation was therefore likely delayed in this valley compared to those with south facing slopes. Studies of glacier responses to climate change from the Cascade and Coastal Mountain Ranges indicate considerable variability between sites, which is also likely in the Southern Rockies (Licciardi et al. 2004; Menounos et al. 2009). Mountain glaciers still exist in the Kananaskis region at elevations higher than the peaks (Mount Smuts, The Fist and Mount Shark) above the narrow valley containing Shark Lake and are known to have advanced during the Little Ice Age (LIA), but did not reach Late Wisconsinin extents. The moraines and lowermost LIA extension of the lowest of these glaciers are above the elevation of Shark Lake (Smith, et al. 1995; Luckman 1994; Luckman 2000).

The Shark Lake catchment is mainly covered in forest consisting predominantly of Lodgepole Pine (*Pinus contorta*) and Engelmann Spruce (*Picea englemannii*) (Johnson and Fryer 1989; MacDonald 1989; MacDonald 1982). European exploration of the Kananaskis Valley was first recorded in 1854, but widespread logging did not begin until 1886. Higher elevations, such as the Shark Lake catchment, may not have been logged until after the 1940s). Early European forest surveys showed fire damage and a forest composition similar to modern (Johnson and Fryer 1987; Johnson and Fryer 1989). The area was designated a Provincial Park in 1977; however, areas nearby are still selectively logged for trail and utility right-of-way maintenance. The Shark Lake catchment itself has not been recently logged (and perhaps has never been logged), and access to the lake is limited to a narrow, forested trail extending from a poorly maintained logging road that ends ~200m from the lake (Figure 5).

The carbonate bedrock contributes to high levels of alkalinity in the inflowing catchment water and in the lake (84 mg/L expressed as equivalent $CaCO_3$). This in turn

leads to authigenic carbonate mineral formation in the water column when primary production by phytoplankton increases during spring and summer and produces a shift in pH toward more positive values (and greater CO_3^{2-} concentrations) (Kelts and Hsü 1978; Thompson et al. 1997; Hodell et al. 1998). Alkalinity is measured as an equivalency of acid to buffer the water to neutral, and high alkalinity is a strong indicator of the potential for authigenic carbonate formation. Satellite images indicate possible whiting events in Shark Lake and other lakes in the region.

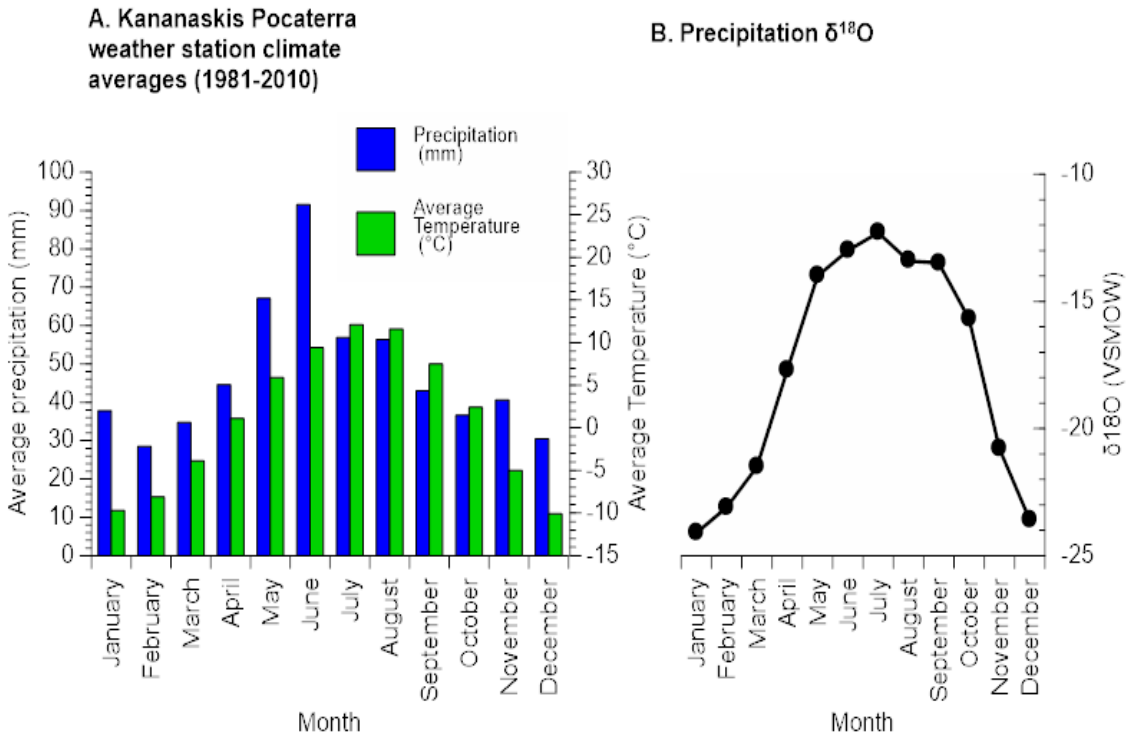

Figure 3 – Precipitation and climate data
A. Monthly average precipitation amounts and average temperature from the Kananaskis Pocaterra weather station from 1981-2010.

The Köppen climate classification of Kananaskis Country is Dfc (subarctic), with cold winters and mild summers. The closest weather station to Shark Lake with a historical record of significant length is Kananaskis Pocaterra, ~25 km to the southeast, at 1,600 m ASL, ~250 m below Shark Lake. Climate data has been recorded there since 1981. The late spring and early summer are the wettest times of year, with May averaging over 60 mm and June over 80 mm of precipitation (Figure 3). Winter precipitation is substantial as well, nearly evenly distributed from November through January. The

minimum average temperature is -10.1ºC in December and the maximum average temperature is 12.1ºC in July, with an average annual temperature of 1.1ºC. In the cold season (months November through April), low temperatures can reach -44ºC, but the daily temperature ranges from -16.5ºC to 7.9ºC. During the warm season (May through October) the maximum recorded temperature is 33ºC, and the daily range is between -4.6ºC and 20.6ºC. Estimated deuterium and ^{18}O isotope ratios of average monthly precipitation (waterisotopes.org) range from -182 and -24‰ (VSMOW), respectively, in January to about -96 and -12‰ (VSMOW) in July (Figure 3). The annual weighted average precipitation isotope ratios are -16.6 and -126 ‰ for $\delta^{18}O$ and δD, respectively (Bowen and Wilkinson 2002; Bowen 2008).

Many paleoclimate studies of North America have focused on solar insolation driven trends and associated hydroclimate responses (Ersek et al. 2012; Asmerom et al. 2007; Hu et al. 2003). Orbital forcing is thought to have produced changes in interannual to multidecadal scale climate oscillations and modes such as the PNA, ENSO, PDO and the NAO (Rodionov et al. 2007; Liu et al. 2014; Bird et al. 2017; Anderson et al. 2016). Hydroclimate in the Rocky Mountains is strongly influenced by storm tracks in all seasons. Synoptic climate oscillations in the Pacific and Atlantic basins affect jet stream circulation and thus seasonal precipitation. Varying in both strength and position on a range of timescales, the Aleutian Low pressure system (AL) is a strong control on atmospheric air circulation in western North America (Rodionov et al, 2007). The cyclonic circulation pattern of the AL drives moist air from the Pacific Basin into the inland Pacific Northwest. During the winter, the Aleutian low strengthens and migrates to the south, with a mean position typically centered over the Gulf of Alaska and/or the Aleutian Islands. During the summer, the Aleutian Low weakens, migrates to the north, with a mean position typically adjacent the western coast of Alaska, and is replaced (in terms of influence) by the North Pacific high-pressure system. Depending on its position, the North Pacific High will block westerly flow from the Pacific basin and prevent moist air from entering North America. The location and strength of the Aleutian Low and North Pacific High on intra- and interannual timescales is controlled by interrelated modes of Pacific ocean-atmosphere variability including ENSO and the PDO and their effects on synoptic scale atmospheric circulation patterns characterized by the PNA.

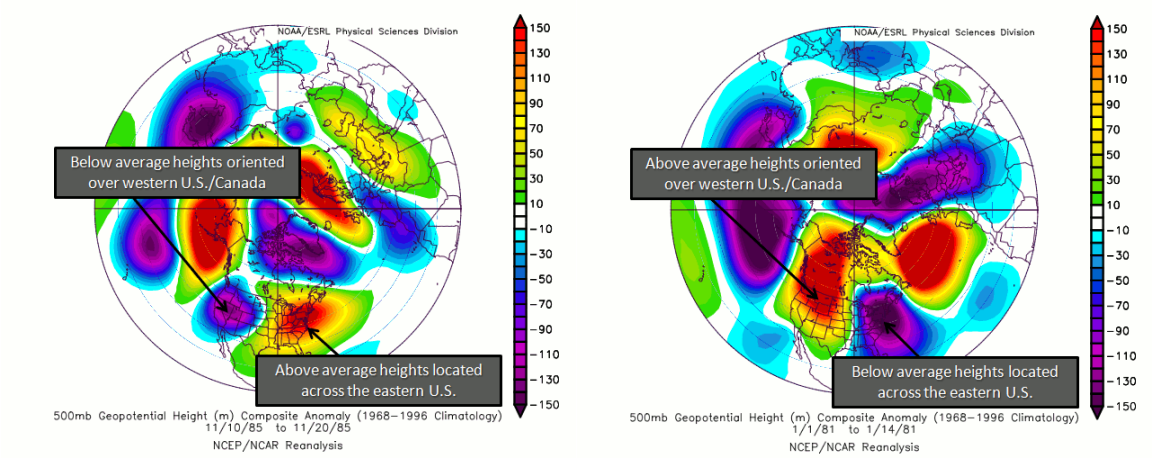

Figure 4 – PNA Patterns
Geopotential heights during negative (left) and positive (right) phases of the PNA. Figures produced by the North Carolina Climate Office and NOAA Climate Prediction Center (obtained from https://climate.ncsu.edu/climate/patterns/pna). The negative phase is associated with greater winter precipitation in the Canadian Rocky mountains.

The PNA, most strongly expressed in winter, is a dipolar interannual mode of 500 mb geopotential pressure heights centered on the North American continent that is modulated by interdecadal / multidecadal trends in the PDO. Essentially, the PNA influences the strength and position of the jet stream and the associated delivery of moist air masses from the Pacific basin to the North American interior. During positive phases of the PNA, the Aleutian Low is stronger and the 500 mb elevation is high above western North America, which leads to a strengthened high-pressure ridge over the Rocky Mountains and warmer temperatures (Figure 4). Precipitation in the northernmost regions of the Pacific Northwest (e.g. northern British Columbia and the Southern Yukon) is typically greater while drier conditions prevail in much of western North America, with the exception of the southwest which exhibits an anti-phased response. That is, the precipitation response to the PNA in the northern and southern regions of western North America is opposite that of the central region. The negative phase of the PNA is characterized by a weaker Aleutian Low, low 500 mb elevations and a weakening of the ridge pattern over western North America (including the Rocky Mountains) and colder winter temperatures. Precipitation amounts are typically greater in much of western North America but lower in the northern region of the Pacific Northwest and the southwest (i.e. opposite the response of the positive phase of the PNA). Other atmospheric pressure patterns that influence North America such as the North Atlantic Oscillation (NAO) and

closely related Northern Annular Mode (NAM) can modify the position of the jet stream in eastern North America as well. A positive NAM phase is associated with a strengthening of the westerlies, leading to reduced delivery of cold arctic air masses to the interior of continental North America; the reverse is true for the negative phase of the NAO, which allows cold air to migrate southward into the continental interior.

Pacific sea surface temperature (SST) variations related to PDO and ENSO can cause a range of changes in atmospheric circulation that can lead to variability in storm tracks across western North America that affect precipitation amounts in the Rocky Mountains. ENSO is an interannual mode of ocean-atmosphere variability (three to seven-year periodicity) centered in the tropical Pacific Ocean that is defined by the pressure difference between the south-central and western regions of the Pacific and SSTs in the eastern region of the basin. The positive phase is characterized by weakened easterly winds in the tropics and warmer SSTs near the coast of South America. The negative phase of ENSO (also known as La Niña) is characterized by strengthened tropical easterly winds, and greater upwelling and colder temperatures along the coast of South America. Negative phases of ENSO and positive phases of the NAM typically produce greater winter precipitation in the Pacific Northwest and northern Rocky Mountains (Steinman et al. 2016), although the spatial patterns of precipitation responses to ENSO are highly variable. Positive phases of ENSO and negative phases of NAM typically cause dry conditions in the Pacific Northwest. The PDO is a pattern of oscillations in north Pacific SST that is essentially the interdecadal / multidecadal expression of ENSO in the north Pacific and thus is technically not an independent mode of variability (Newman, Compo, and Alexander 2003). Both ENSO and PDO are strongly connected to the PNA, in that they reflect variability in different components of the Pacific ocean-atmosphere system and on different timescales.

On a continental scale, the PNA is strong control on spatial and temporal patterns of variability in the isotopic composition of precipitation. The northwest region of North America typically exhibits a response opposite that of the southwest during phase changes of the PNA, while the southern and eastern regions of North America typically change in concert with the southwest (Liu et al. 2014). The result is that during positive

phases of the PNA, precipitation isotope values are generally more positive in the west-central and northwestern regions of north America and more negative in the southwestern, south-central and eastern regions of North America.

3. Methods

3.1 Water Stable Isotope Analysis

In 2015, 2016, and 2017 water samples from surface water bodies were collected in 30 mL polyethylene bottles after rinsing three times with sample water and then filling and capping the bottle underwater. All samples were stored in cool (~4 °C), dark conditions until analysis. Isotopic ratios of the water samples (supplemental data Table 5) were measured either at the University of Minnesota Duluth or at the Indiana University Purdue University Indianapolis (IUPUI) Department of Earth Sciences on a Picarro L2130-i Analyzer coupled to an autosampler and high-precision water vaporizer unit (Bird et al. 2011). Water isotope measurements were corrected for memory and drift using calibrated standards from Los Gatos, and precision for δD and $\delta^{18}O$ is 0.6 ‰ and 0.1 ‰, respectively. All water isotope results are reported in standard delta notation relative to Vienna Standard Mean Ocean Water (‰ VSMOW). Monthly precipitation isotope data was obtained from waterisotopes.org (Bowen and Wilkinson 2002; Bowen 2008).

3.2 Alkalinity

Alkalinity was measured in 2016 using a Hach titration kit in the field. Lake water was combined Bromcresol green-methyl red indicator powder and acidified using 1.6 N sulfuric acid. Alkalinity is reported as of equivalent $CaCO_3$ (mg/L) and reflects the total dissolved bicarbonate and carbonate concentration (Kelts and Hsü 1978).

3.3 Sediment Core Collection

Sediment cores were collected from near the center of the lake, rather than the shallow surrounding shelf since increased clastic input and sediment disturbance is likely near shore. Areas near the steep slope from the shallow shelf (~1 m depth) to the nearly uniform deep portion (~4 m) were avoided due to a risk of subaqueous mass wasting, which could disturb the sediment stratigraphy.

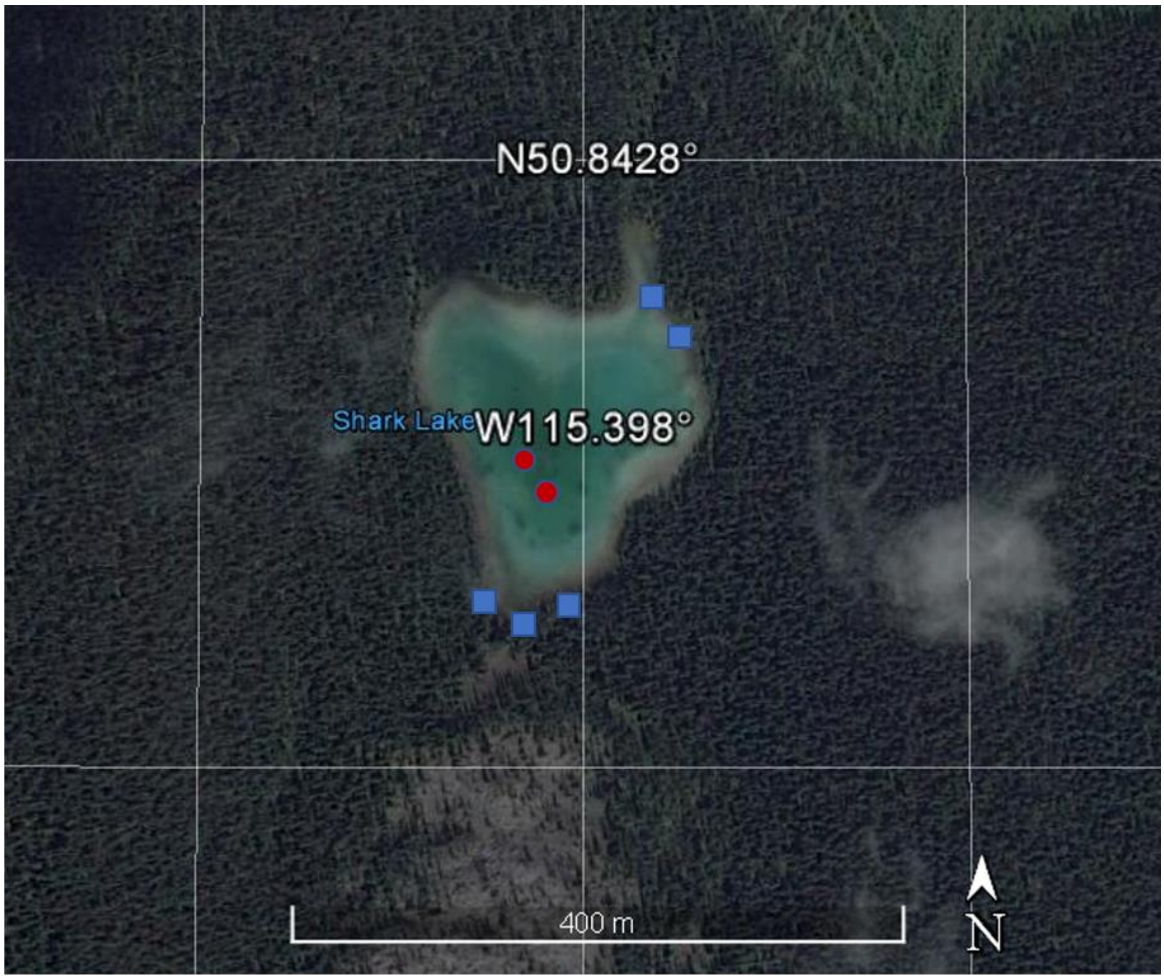

Figure 5 – Sample Locations
Sample locations from 2016 and 2017 coring and water sampling. Several water sampling locations were used both years Additional water samples from the region were collected, see supplemental data.

During both 2016 and 2017, cores were collected at a depth of 4.3 m using a modified Livingstone corer fitted with a 6.7 cm polycarbonate barrel (Wright et al. 1984). A 1.5 m Bolivia-type core was also collected in 2016 using the Livingstone square rod and a polycarbonate tube (6.7 cm diameter). In July 2017, one-meter long sediment cores were collected from Shark Lake using a modified Livingstone piston corer with a five cm diameter steel barrel. The uppermost 30 (2016) to 40 (2017) cm of sediment was transferred to sterile plastic bags via upward extrusion in 0.5 cm increments into a tray fitted to the top of the core barrel. The Livingstone cores were extruded in the field into

ABS plastic tubes lined with plastic wrap and sealed. Cores collected in polycarbonate were capped and sealed as well. All cores were stored in refrigerated (~4° C) cold rooms at the University of Pittsburgh and the University of Minnesota Duluth until the time of splitting and sampling. The Shark Lake sediment cores are labeled as follows: Surface Core A16, Bolivia Core D1 A16, Surface Core A17 and Livingstone cores A17 D1-D5.

3.4 Core splitting, imaging, and XRF scanning

At the University of Pittsburgh, sediment cores were split in half length-wise using a metal blade. Immediately after opening, one cm^3 samples were collected at two cm resolution for loss-on-ignition (LOI) analysis using a custom stainless-steel plunger. The split cores were imaged at the University of Pittsburgh using a Geotek Multi Sensor core logger at 10 pixels per mm. Terrestrial plant macrofossils were collected for radiocarbon analysis using a paintbrush and tweezers cleaned with methanol. The Mazama tephra layer was identified for absolute dating by visual inspection and texture.Split cores were scanned at the University of Minnesota Duluth using an ITRAX X-ray fluorescence (XRF) core scanner for elemental ratios using florescence to estimate atomic abundance. The scanning resolution was 0.5 mm intervals with a dwell time of 15 seconds per sample point. Radiation parameters were set to a maximum voltage of 60 kV and maximum current of 30 µA, with a Cr source tube and an exposure time of 200 msec. XRF results were correlated with oxygen isotope results from sliced samples and normalized to coherent scatter from chromium.

3.5 Loss-on-ignition

Loss-on-ignition analysis was conducted at the University of Minnesota Duluth. Samples were initially dried using either a Labconco freeze drier or a drying oven set at 100°C for 48 hours, weighed, then placed in pre-weighed ceramic crucibles and combusted in a Thermolyne Furnatrol 53600 muffle furnace at 550°C for four hours. Samples were weighed again then combusted at 1000°C for one hour. Composition after the 550°C combustion was determined by mass loss of organic matter from the dry weight after removing container weight. After the 1000°C combustion, the total mass of $CaCO_3$ was calculated by first determining the mass loss between the 550°C and 1000°C

burns and multiplying this value by the stoichiometric mass ratio of 100/44 ($CaCO_3/CO_2$) (Heiri el al. 2001).

3.6 Sediment chronology

Terrestrial plant macrofossils collected for radiocarbon (^{14}C) analysis were cleaned under a microscope using deionized water and a paintbrush and refrigerated (~4° C) until analysis. Pretreatment and combustion for ^{14}C were conducted at Northern Illinois University using a standard acid-base-acid treatment (Abbott and Stafford 1996). Analysis for ^{14}C was conducted at the University of California Irvine via AMS following the procedure of Donahue, et al. 1990. Ages were calibrated to years BP with the program CALIB 5.1 with the calibration dataset IntCal13 (Stuiver and Reimer 1993; Reimer et al. 2013).

At the University of Pittsburgh extruded surface samples spanning 0-15 cm were lyophilized, weighed, and sealed in airtight petri dishes for three weeks prior to analysis for lead-210 (^{210}Pb) and cesium-137 (^{137}Cs) dating. The samples were measured for 48 hours using direct gamma counting on a Canberra BE-3825 high-purity, broad-energy germanium detector. Results were interpreted using the constant rate of supply (CRS) method (Appleby and Oldfield 1983).

Bchron, a Baysesian statistical age-model software package for R (Haslett and Parnell 2008; Parnell et al. 2008; Parnell, et al. 2011), was used to produce a median age and probability distribution (2σ uncertainty range) for each depth increment on the basis of the age control point data, which include the depth interval spanned by the sample, the calibration curve, and the AMS measurement uncertainty. The IntCal13 calibration curve (Reimer et al. 2013) was applied to estimate radiocarbon age uncertainty, and normal distributions were assumed for uncertainty in the ^{137}Cs and ^{210}Pb control points.

3.7 XRD and SEM

Sediment mineral composition was determined via X-Ray Diffraction (XRD) using a Philips X'Pert X-Ray diffractometer. Representative samples were taken at least every 50 cm to determine carbonate mineral phase; seven samples were analyzed in total. Samples were treated with hydrogen peroxide (7% v/v) and sieved through a 63-micron screen. The fine fraction was collected, bleached with 15% v/v sodium hypochlorite,

rinsed three times with deionized water, then freeze dried. The carbonate mineral phases were identified to determine if calcite or aragonite were present since they have different isotope fractionation factors (Kim and O'Neil 1997; Kim et al. 2007). Silicate minerals were categorized as minerogenic clastic material. Sediment was viewed under a JEOL JSM-6490LV scanning electron microscope (SEM) to assess the extent of detrital calcite contamination resulting from catchment erosion. Samples were set using carbon tape and coated in graphite then viewed using the SEM to between 1,200 and 1,700 times scale. Visible carbonate and silicate grains were searched for since diatoms were plentiful and adhered to carbonate sediment.

3.8 Core sampling and isotope analysis

Sediment cores were sampled at 0.5 cm resolution using a custom-made core slicing device. Samples were prepared for oxygen isotope analysis at the University of Minnesota Duluth using the method (described above) applied to the XRD samples. Analyses were conducted at the University of Arizona Environmental Isotope Laboratory using a Finnigan-MAT Kiel III carbonate preparation device coupled with a Finnigan-MAT 252 mass spectrometer. Samples were digested using orthophosphoric acid at 70° C. Measurements were calibrated to the NBS-18 and NBS-19 calcite standards and values are reported in standard delta notation as the per mil deviation from Vienna Pee Dee Belemnite (VPDB). Replicate sample analyses were performed on approximately 10% of samples.

3.9 $\delta^{18}O$ record correlation analysis

A Monte Carlo based analysis that accounts for age model uncertainty based on the age model results was applied in order to assess the correlation between the Shark lake $\delta^{18}O$ record and other open-basin lake and speleothem $\delta^{18}O$ records from North America (Table 2). One thousand realizations of each age models were produced for each record using age control point data (^{14}C, ^{210}Pb, ^{137}Cs measurements for lake records and $^{230}Th/^{234}U$ ages for the speleothem records) and the Bchron age-model software package, resulting in 1000 different realizations of each $\delta^{18}O$ record. For each correlation assessment, 1000 correlation (Pearson's r) and significance (p) values were calculated for each combination of realizations of the Shark Lake record and records from the other

study sites (e.g. 1000 r and p values were produced for the Shark Lake and Lime Lake assessment). Two-σ limits of the resulting distributions of r and p values were calculated in order to assess similarity between the records. Correlation significance was assumed for p distributions for which the upper 2-σ limit (p range=0.98) was less than 0.1. The r values determined if the correlation was positive or negative. This analysis was conducted after 10-year interpolation was applied to each realization of each record as well as low-pass filtering across a range of periodicities in order to assess the correlation and significance of low frequency signals in the datasets. Low-pass filter periods of 10, 50, 100, and 500 years were applied using the adaptive low-pass filter of Mann 2008.

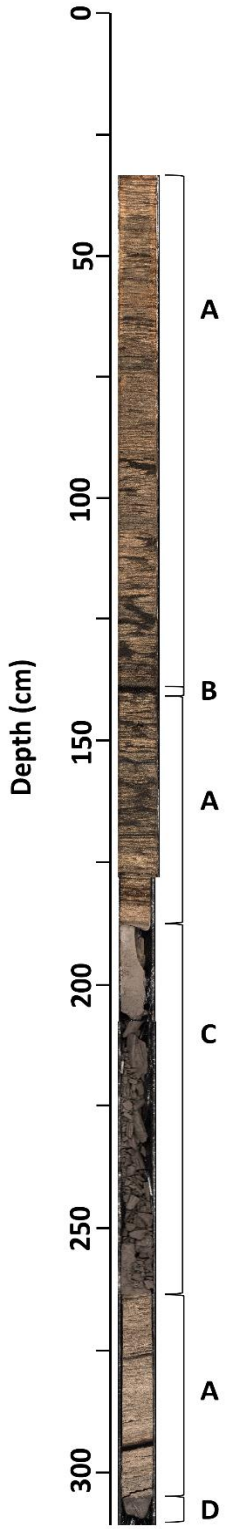

Figure 6 – Stratigraphic Column
The Shark Lake core sequence from images of multiple drives spliced using stratigraphic markers. Units A-D were classified based on sediment texture (mud, sand or tephra), mineral content and visual stratigraphic changes.

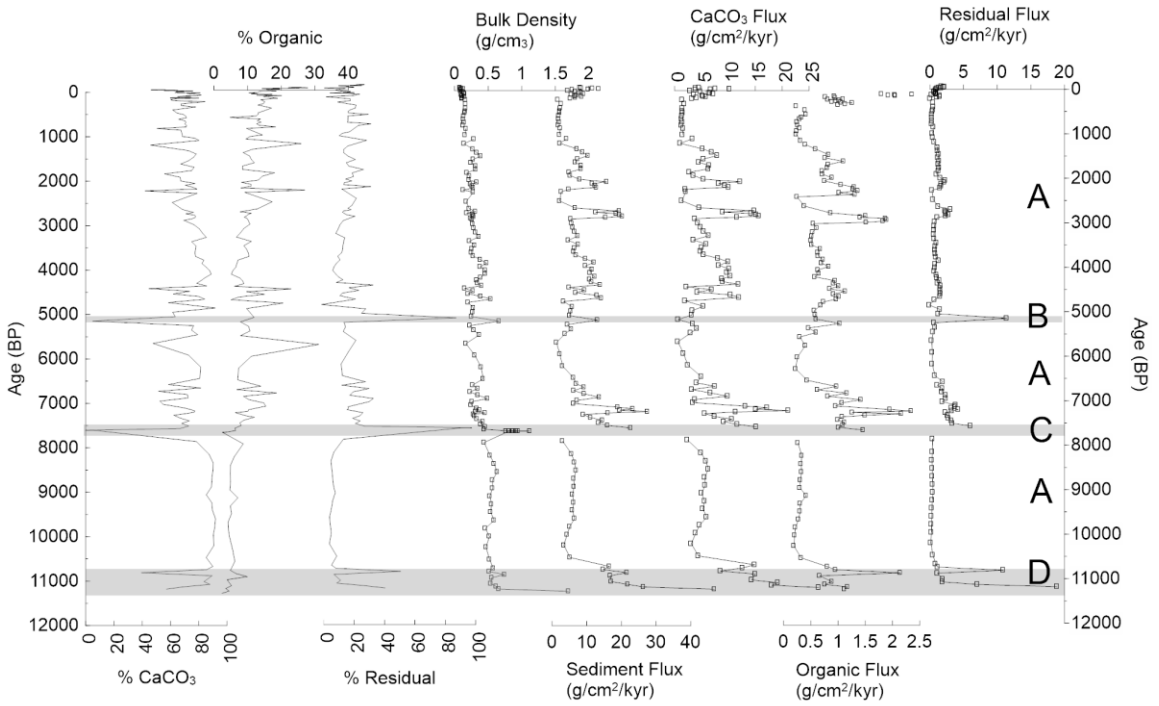

Figure 7 – Loss on ignition, bulk density and sediment fluxes
Bulk sediment composition and density are used to identify minerogenic layers. Total sediment flux and component flux show changes in sedimentation rate and composition. The gray boxes represent clastic sediment layers.

4. Results

4.1 Sediment Lithology

The sediment cores are made of three main sediment categories: carbonate mud, tephra, and glacial clay (Figure 6). Spanning depths of 0-135 cm, 137-189 cm and 263-306 cm, Unit A is the primary sediment type, consisting of fine grained, tan carbonate mud with dark brownish-gray mottling and banding (Figure 6). For Unit A, the carbonate mineral content is between 50% and 85% (by mass), organic matter is between 7-25%, and residual mineral amounts are 5-35% (Figure 7). Some of the dark layers in Unit A extend across the width of the core; however most are not perfectly horizontal. LOI results do not show major compositional differences between darker and lighter sections. Scanning electron microscope images indicate that most of the residual mineral matter is from silicate diatom frustules, which range in size from five to 75 µm and are mainly circular or oblong in morphology. This indicates that there are multiple diatom genera in Shark Lake (Figure 9).

Terrestrial macrofossils, mainly charcoal, are found throughout Unit A . The carbonate mud in this layer is predominantly authigenic calcite, confirmed by SEM images of the mineral crystals and XRD analysis (, Figure 9). Both calcium (Ca) from XRF analysis, and carbonate content (LOI) are relatively higher in the lowest Unit A (263-306 cm) compared to those above the Mazama tephra (Figure 7, Figure 10).

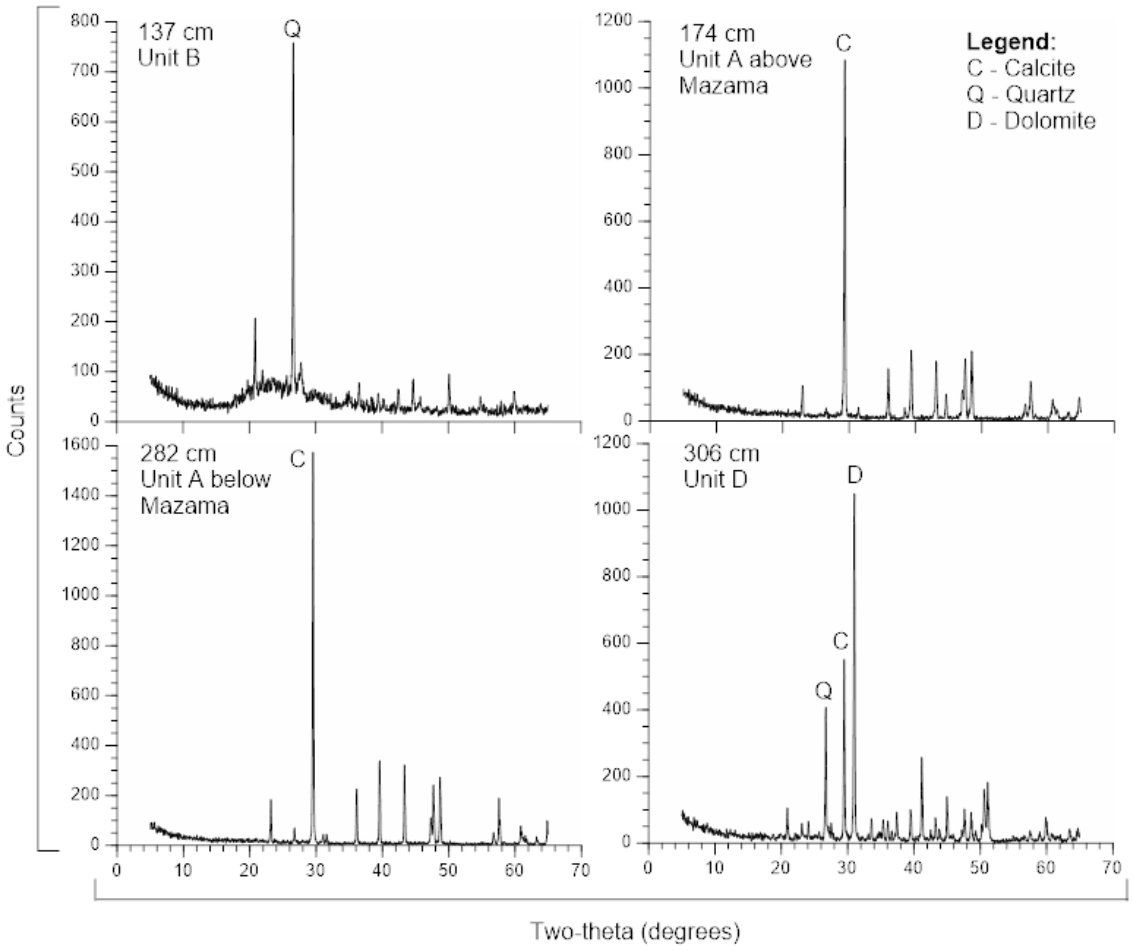

Figure 8 – X-ray diffraction
Mineral phase is shown based on x-ray diffraction angle (two-theta). Peaks were identified for general mineral classification. Clastic layers are higher in quartz and dolomite while authigenic layers are nearly completely calcite. Unit B and D contain more clastic material, Unit A is calcite and shows the same mineral phase both above and below the Mazama tephra.

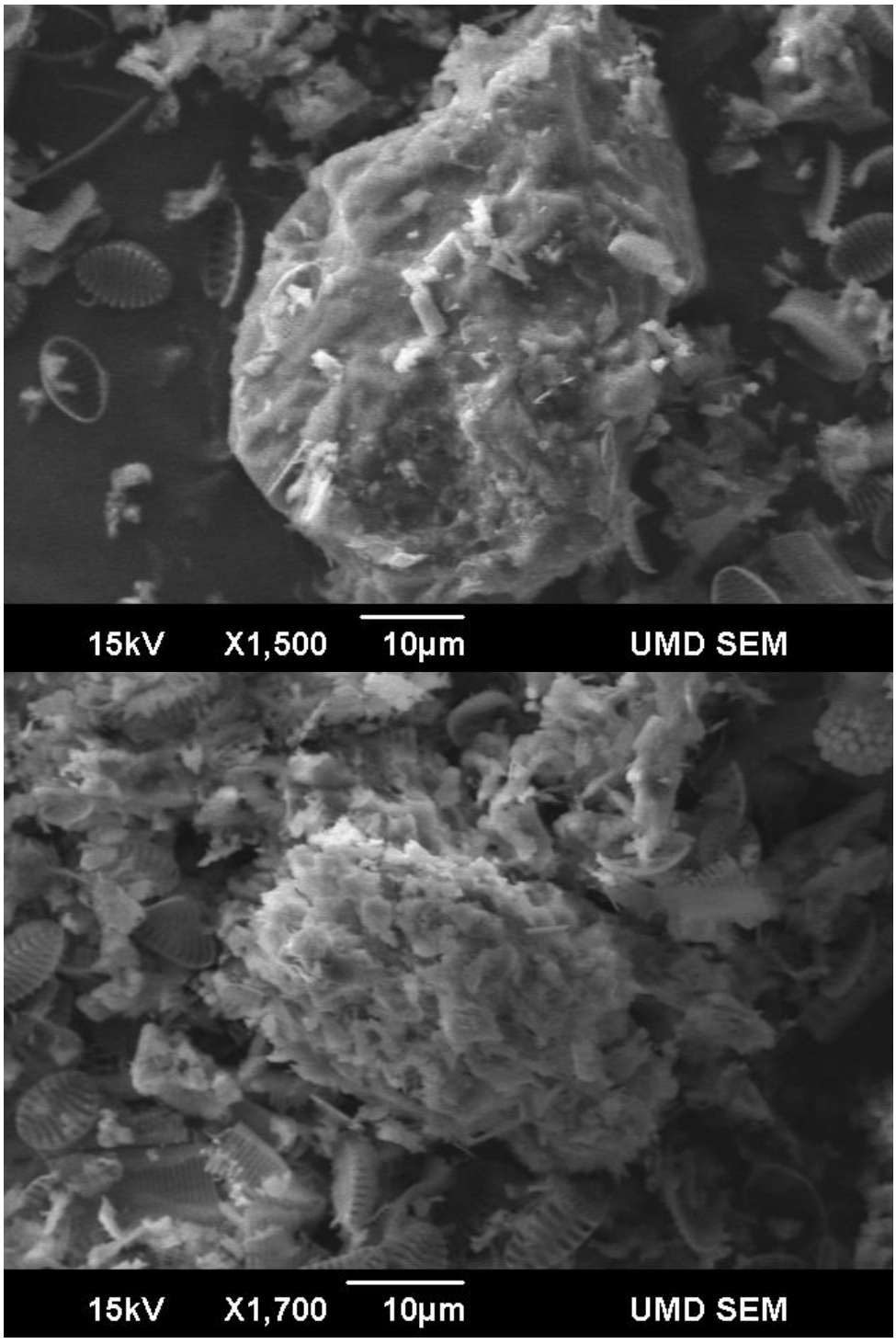

Figure 9 – Scanning electron microscopy

A. An authigenic calcite crystal from Unit A
B. A calcite crystal surrounded by diatom frustules

Unit B is dark in color, similar to the dark brown banding present in Unit A but has a coarse texture and contains around 70 to 90% residual mineral matter (Figure 7) This layer contains some sand-sized grains in a silt matrix. Unit B spans 136-137 cm in the core and has an age of ~5,100 calendar years before present (yr BP) (Figure 11). Elements related to clay minerals like titanium (Ti), silicon (Si), iron (Fe) and potassium (K) showed increased counts on the XRF compared to Unit A (Figure 10).

Unit C spans 189-263 cm and is a light to medium gray, fine-grained (silt sized) clastic sediment with over 90% residual mineral matter and less than 5% carbonate (Figure 6, Figure 7). We determined this layer to be the Mazama tephra on the basis of its thickness, appearance, the bracketing radiocarbon ages, and the consistency of its characteristics with descriptions of the Mazama tephra from other nearby locations (Figure 11) (Beierle et al. 2003; Leonard and Reasoner 1999; MacDonald 1982; Reasoner et al.1994). Large terrestrial macrofossils were found within the tephra, as well as directly above and below the unit. The substantial thickness of the Mazama deposit in Shark Lake is likely due to the steepness and large size (relative to the lake) of the catchment. The Mazama tephra has a radiocarbon age (uncalibrated) of 6,730 ± 40 ^{14}C yr BP which calibrates to 7,597 calendar yr BP (Hallett et al. 1997), and a second age based on layer counting of the GISP2 ice core of 7627 ± 150 yr BP (Zdanowicz, et al. 1999). These ages are consistent with one another, and we apply the radiocarbon age of the Mazama tephra in the Shark Lake age model. XRF results show increases in clay related elements and also sulfur (S) (Figure 10).

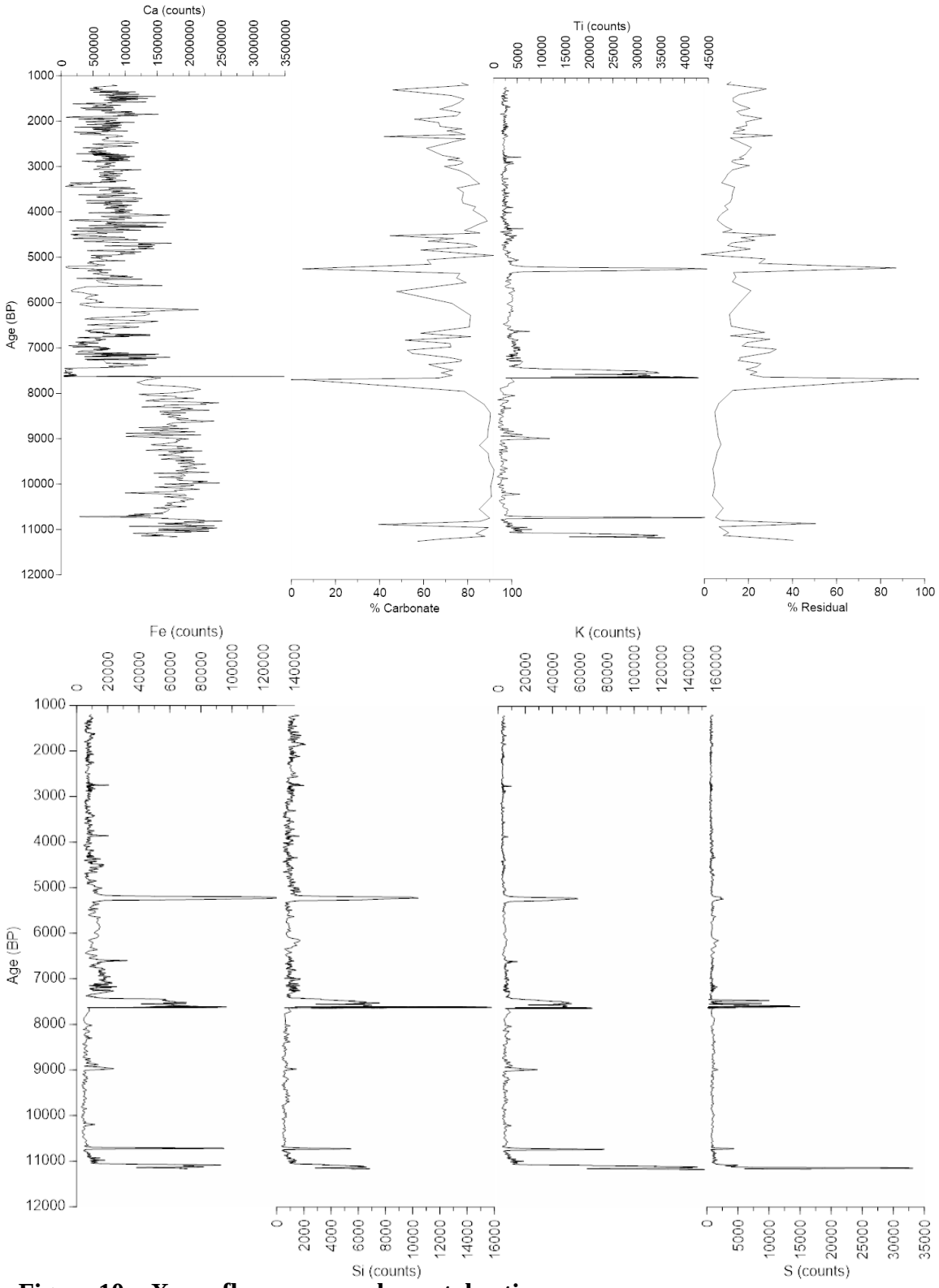

Figure 10 – X-ray fluorescence elemental ratios
Top: Ca and Ti counts compared to % carbonate and % residual.
Bottom: Counts of other common elements found in the sediment that follow clastic deposition.

Unit D is a light gray, very fine grained, clay sized sediment found at the base of the core, spanning 306-313 cm (Figure 6). This layer contains 25-40% residual mineral matter, 57-68% carbonate, and 2-5% organic matter. The texture of unit D is consistent with clay and is likely rock flour resulting from glacial erosion during the early Holocene ice retreat from the depression Shark Lake is in, above the Spray Lake Valley. This assertion is supported by studies of lakes at lower elevations in the greater Kananaskis Valley area, which found abundant, fine clastic sediment at the base of lake sediment sequences with ages of ~10,500 yr BP, similar to the basal age of the Shark Lake sequence (Beierle et al. 2003; MacDonald 1982). XRD and XRF data also supports this layer as eroded country rock as mineral phase contains quartz, dolomite, and calcite while clay related elements and calcium are higher than Unit A, showing deposition of weathered carbonate and silicate rocks (Figure 8, Figure 10).

4.3 Chronology

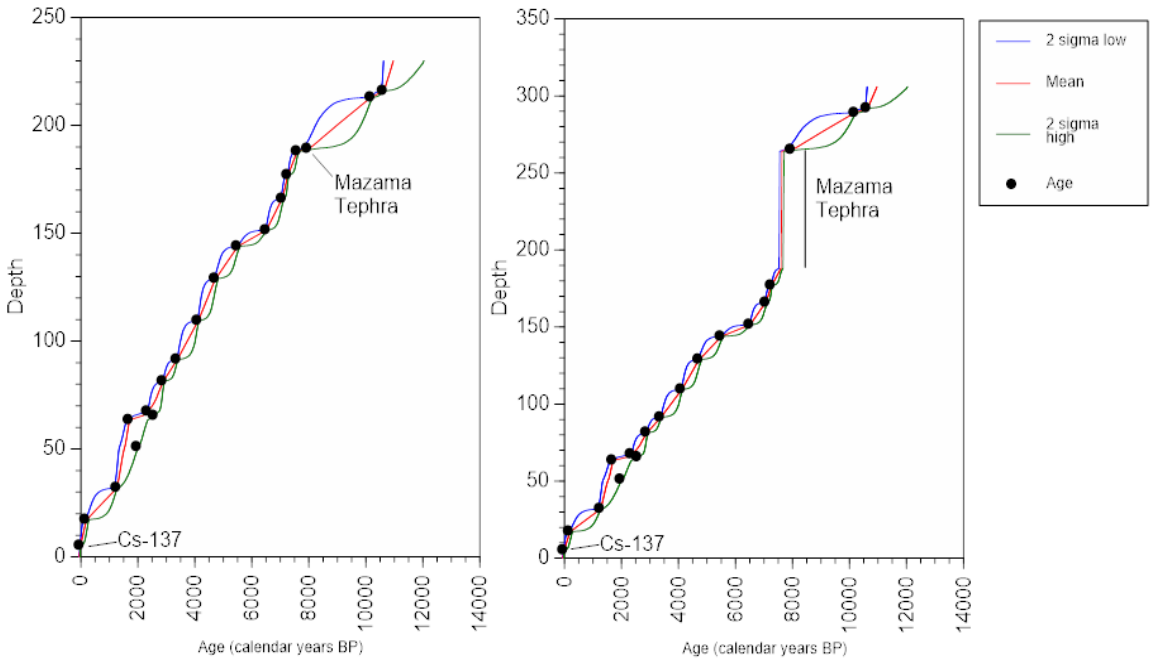

Figure 11 – Bchron age model
Ages from ^{14}C, ^{137}Cs, and the Mazama tephra are shown as the black control points. The right graph shows the age model with the Mazama tephra included, while the left has the tephra removed.

Depth from sediment surface (Mazama tephra removed) (cm)	Sample Material	^{14}C Raw age (BP)	Analytical error for raw ages (±BP)	Median calibrated age (BP)	2 σ low calibrated age (BP)	2 σ high calibrated age (BP)
17.25	Wood	165	20	187	0	284
32	Wood	1315	15	1272	1187	1290
51	Charcoal	2045	20	1999	1934	2105
63.5	Wood	1785	15	1706	1623	1807
65.5	Wood	2505	20	2582	2492	2727
67.5	Wood	2355	15	2353	2339	2369
81.5	Wood	2790	20	2891	2808	2955
91.5	Wood	3165	15	3387	3360	3444
109.5	Wood	3755	15	4120	4011	4219
129	Wood	4175	15	4727	4629	4828
144	Charcoal	4800	20	5509	5477	5592
151.5	Wood	5725	20	6512	6445	6618
166	Needles	6175	20	7079	7005	7161
177	Wood	6335	20	7267	7178	7315
189.25	Wood	7140	170	7967	7666	8322
213	Charcoal	9020	60	10195	9919	10271
216	Charcoal	9295	40	10627	10517	10716

Table 1 – Radiocarbon data

Carbon-14 ages and depths are shown in Figure 11 and Table 1, with the ^{137}Cs ages from the surface sediment and the Mazama tephra as an absolute date. The age model yields a sedimentation rate of about 0.1 mm/yr from Unit D to the Mazama tephra layer (Unit C). The sedimentation rate is higher from the Mazama tephra to the surface of the core at around 0.23 mm/yr. The sediment fluxes of all components are all higher after the Mazama tephra, notably carbonate and organic matter (Figure 7). There may be one age reversal around 60 cm, which is seen in the difference between the 51 and 63.5 cm ^{14}C samples (which are separate by ~300 years) (Table 1). A reversal could be indicative of subaqueous slumping which causes a repeat in sediment deposition. Another explanation is the organic matter was retained on land before burial in lake sediment.

The ^{210}Pb age model was produced using the constant rate of supply (CRS) method (Appleby and Oldfield 1983), but the results were not applied to the age model because of the large uncertainty range, for example, ± 31 years (one sigma) at a depth of 6.25 cm (supplemental data Table 8). The distinct ^{137}Cs maximum at 5.25 cm is assumed

to be 1964, the year after the atmospheric nuclear testing ban, and is consistent with the ^{210}Pb age of 1954 ± 14 years (one sigma) at this depth (supplemental data Table 8).

4.4 Water isotopes

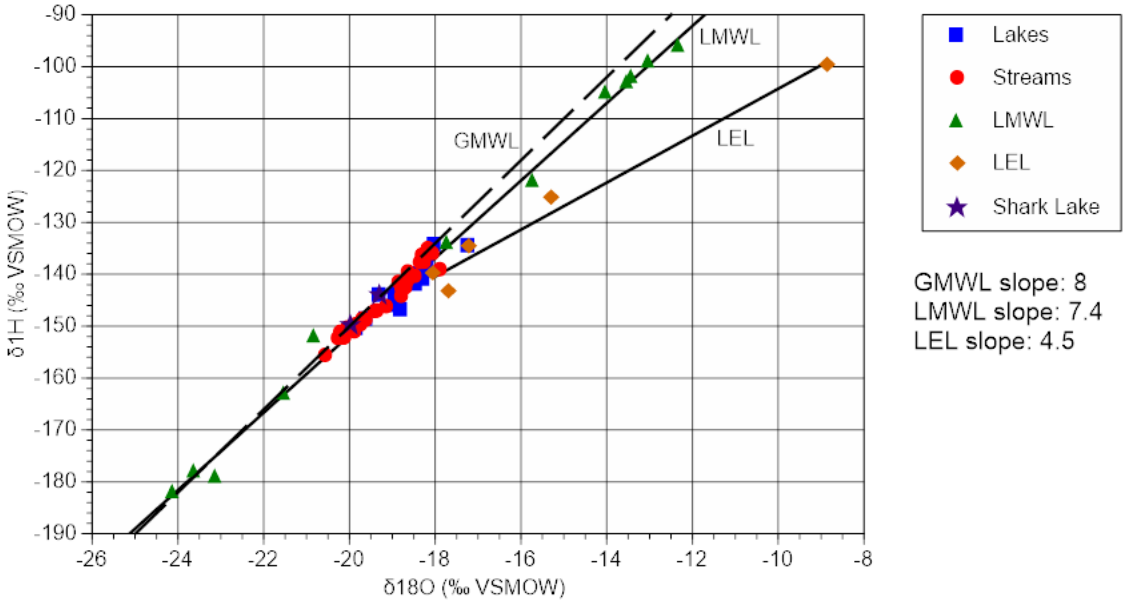

Figure 12 – Water isotope measurements
Water samples collected from surface water in the area with Shark Lake noted. The local meteoric water line (LWML) is made up of precipitation isotope measurements from waterisotopes.org (Bowen, 2008). The closed-basin lakes define the local evaporation line (LEL). The open surface water bodies like rivers and lakes show isotope measurements close to average precipitation values.

Water isotope values of streams varied between -17.9 and -20.6 ‰ for δ^{18}O and -135 to -156 ‰ for δD. Lake values varied between -8.9 to -20.6 ‰ for δ^{18}O and -100 to -151 ‰ for δD; the more enriched values being from hydrologically closed lakes. Shark Lake values samples in August 2016, June 2017 and August 2018 varied from -18.9 to -20.0 ‰ for δ^{18}O and -142 to 150 ‰ for δD (supplemental data Table 5)

The isotopic composition of water from Shark Lake is consistent with that of local meteoric water, which indicates that Shark Lake is an open-basin system with water isotope values controlled by the isotope content of precipitation on the catchment (Figure 12). The Shark Lake water isotope values plot along the local meteoric water line (LMWL), which is established by the isotope values of other local open-basin lakes and streams. The slope of the LMWL is 7.4, which is slightly shallower than the global

meteoric water line (GMWL) slope of ~8. Several lakes have water isotope vales that diverge from the LMWL, which shows they are influenced by evaporation. Values from these lakes plot along the local evaporation line (LEL), which has a slope of 4.5.

The annual weighted average precipitation isotope ratios are -16.6 and -126 ‰ for $\delta^{18}O$ and δD, respectively. The collected samples from Shark Lake are more depleted than the precipitation from both the months in which were collected and the annual weighted average meteoric values. This shows that the water sourcing Shark Lake is derived from winter snowpack or groundwater from higher elevations and that the water balance of the catchment is controlled by winter precipitation.

4.5 Sediment Isotopes

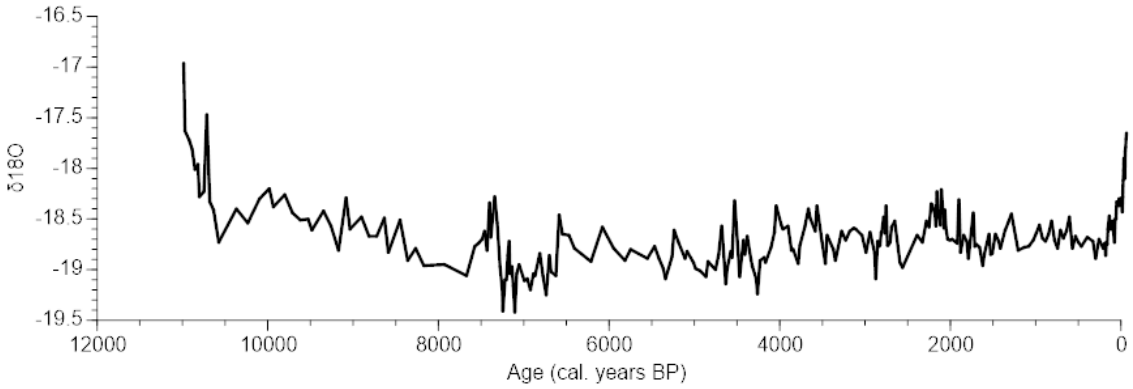

Figure 13 – Lacustrine carbonate $\delta^{18}O$ record
The Shark Lake $\delta^{18}O$ record begins around 11,000 yr BP with enriched $\delta^{18}O$ values. There is a marked shift between the middle and lake Holocene at ~7500 yr BP, from a decreasing to an increasing trend.

Shark Lake sediment oxygen isotope ratios generally decrease from ~9,000 to 6,200 cal. yr. BP then increase from 6,200 yr BP until present. There is a marked change in the rate of increase in the samples at the very surface. The most enriched results occur at 9,000 yr BP and in modern sediment, with values of -17.3 ‰ and -17.7 ‰, respectively. The most depleted values of -19.4 ‰ occur at 7,300 to 7,400 yr BP.

The $\delta^{18}O$ values of Shark Lake sediment are approximately consistent with expected theoretical values determined using the estimates of lake water temperature and the calcite-water oxygen isotope fractionation relationship. For example, Shark lake average sediment $\delta^{18}O$ values are -18.65 ‰, which is consistent with the theoretically predicted range of -18.1 to -19.6 ‰, assuming a water/calcification temperature range of

8-15 °C. The surface sediment values fall slightly outside of this range, likely due to catchment destabilization (perhaps associated with logging) and the consequent contamination of Shark Lake surface sediment with detrital carbonates. The $\delta^{18}O$ values (-17.0 to -18.3 ‰) at the base of sediment sequence, which are likely partially reflective of the values of glacial clastics, are approximately consistent with values at the top of the surface sediment (-17.6 ‰).

5. Discussion

5.1 Proxy Background

Analyses of lake sediment cores have provided information on past changes in terrestrial climate from many locations throughout the world. A wide range of biological and geochemical proxies offer insight on lacustrine paleo-environments, including the analysis of pollen, sediment lithology, diatoms, organic matter biogeochemistry, and carbonate sediment isotope values, among others. Pollen analysis can indicate large-scale land cover changes such as transitions in ecotones, while sediment lithology can reveal changes in the sources of sediment as well as variations in lacustrine deposition settings, for example, related to lake level (Davis and Botkin 1985; Anderson et al. 2015; Williams et al. 2010). Organic matter biogeochemistry and the abundance and species composition of diatoms can demonstrate shifts in lake and catchment biological parameters as well water chemistry changes (Bird et al. 2014; Whitlock et al. 2012). Carbonate sediment isotope analysis can provides a record of past changes in lake water isotope values, which are influenced by influence of precipitation and evaporation on lake/catchment hydrology as well as changes in the isotopic composition of precipitation (Steinman et al. 2016). Such datasets can be used to produce records of ocean-atmosphere processes and local catchment hydrologic balance (Bird et al. 2014), and can also be compared with marine sediment records to assess the timing of terrestrial environmental changes in the context of ocean-atmosphere teleconnections or major, global scale changes in climate such as marine isotope stages (Finkenbinder et al. 2016; Kim et al. 2004; Liu et al. 2014).

5.2 Isotope Background

Oxygen has three isotopes, all of which are stable. Oxygen-16 is the most abundant isotope at 99.76%, while oxygen-17 and oxygen-18 make up only 0.04% and 0.2%, respectively. We focus on the ratio between oxygen-18 compared to oxygen-16 in water and sediment. The standard used for solid carbonate samples is Vienna Pee Dee Belemnite (VPDB), and the standard used for water samples is Vienna Standard Mean Ocean Water (VSMOW). Differences between oxygen-18 concentrations in samples are typically very small and are therefore expressed in per mil notation (see equation below), which is analogous to a percentage only with a base of 1000.

$$\delta^{18}O‰ = \frac{\left[\left(\frac{^{18}O}{^{16}O}\right)sample - \left(\frac{^{18}O}{^{16}O}\right)standard\right] \times 1000}{\left(\frac{^{18}O}{^{16}O}\right)standard}$$

Natural processes involving phase changes in water lead to isotope fractionation in water reservoirs. Water molecules with lighter isotopes of oxygen and hydrogen are preferentially removed from liquid water by evaporation though equilibrium and kinetic fractionation processes, and are preferentially retaining in the vapor phase during condensation through equilibrium fractionation processes alone (Gat 1996). The hydrogen bond strengths between water molecules containing either heavier isotope (^{18}O or ^{2}H) are stronger, which means it takes a greater amount of energy to break the bonds for these molecules to evaporate. During phase changes from vapor to liquid (and liquid to solid), the heavier isotopes tend to concentrate in the liquid (solid) phase due to greater hydrogen bond strengths associated with the heavier isotopes. Water isotope values of precipitation plot along a meteoric water line with a slope value of approximately eight (Figure 12) (Bowen and Revenaugh 2003). This implies eight-fold greater isotope fractionation of hydrogen than oxygen during equilibrium fractionation between the vapor and liquid phases in the atmosphere, which is due to the greater hydrogen bond strengths between molecules containing ^{2}H versus those containing ^{18}O. Water bodies that have been substantially influenced by evaporation will plot along an evaporation line that intersects the local meteoric water line and has a lower slope of approximately four

to six. This lower slope is due to greater kinetic fractionation of water molecules containing ^{18}O versus ^{2}H during the process of evaporation.

Rayleigh fractionation is the process that causes progressive isotopic depletion of both oxygen and hydrogen isotopes in air masses during cooling, condensation and rain out (Rozanski et al 1992). Initially, the isotopic composition of precipitation is relatively heavy due to greater abundance ^{18}O in the air masses, which are typically sourced from evaporation over the ocean. As atmospheric temperatures decline, precipitation occurs, and the heavier isotope is preferentially removed from the air mass. Warm season precipitation tends to be enriched in heavy isotopes compared to winter precipitation due to enriched source water and higher atmospheric temperatures and thus higher saturation vapor pressures (moisture capacity of the atmosphere), which lead to less overall isotopic fractionation. The opposite is true during the cold season. Average meteoric water isotope values are based on seasonal precipitation isotope values and amounts, with more winter precipitation leading to lower annual $\delta^{18}O$ on average (Figure 3, Figure 12). In the middle and high latitudes isotope values in precipitation are strongly controlled by temperature through Rayleigh distillation; however, in the tropics rainfall amount effects are the strongest isotopic control, and temperature effects are secondary (Stansell et al. 2013).

δD and $\delta^{18}O$ of lake surface water can be compared to local meteoric water values to determine the extent of evaporation on the lake hydrologic budget (Li and Ku 1997). Changes in lake water isotopic composition are controlled by inflowing meteoric water isotope values and lake hydrologic properties (Gat 1996). In lakes with short residence times, due to high flow-through rates and minimal water losses via evaporation, lake water isotope ratios are typically close to those of precipitation, with a bias based on the amount of precipitation in each season and evapotranspiration rates from surface soils. Lakes with water isotope values close to precipitation tend to have an open-basin hydrologic configuration with active outflows and/or high rates of groundwater through flow. Isotope values of open-basin lakes plot along the LMWL; their water isotope content is influenced by equilibrium fractionation during atmospheric processes and most importantly is minimally affected by evaporation from the lake. Hydrologically closed lakes that lose significant amounts of water through evaporation concentrate the heavier

isotopes of oxygen and hydrogen relative to lakes that do not lose substantial water through evaporation. Water samples from these lakes plot along a local evaporation line (LEL) that diverges from the LMWL, with a shallower slope due to greater kinetic fractionation of oxygen compared to hydrogen (as discussed above). A main consequence of these relationships is that in closed-basin lakes meteoric water isotope values provide the baseline for subsequent isotopic modification by evaporation.

Authigenic carbonate sediment oxygen isotope ratios are reflective of lake water isotope values, with a secondary influence by the water temperature at the time of calcification (Kim and O'Neil 1997). The equation from Kim and O'Neil (1997):

$$1000*1n\alpha(\text{Calcite-}H_20) = 18.03\ (10^3 T^{-1}) - 32.42.$$

relates the calcite-water fractionation factor (α) to lake water temperature. Carbonate sediments from open-basin lakes capture trends in meteoric water inflows, mainly the seasonality of precipitation, as the $\delta^{18}O$ of precipitation changes by about 0.6‰ per °C of surface temperature in mid-latitudes (Rozanski et al 1992; Dansgaard 1964). Closed-basin lake carbonate mineral isotope values are most strongly controlled by the balance between evaporation and precipitation, with more positive values occurring during drier conditions and vice versa. The $\delta^{18}O$ values of carbonate sediment in open-basin lakes can therefore provide records of precipitation and meteoric water isotope values that, in addition to providing information on broad scale atmospheric processes, can be subtracted from closed-basin lake carbonate $\delta^{18}O$ values in order to isolate the hydrologic balance (precipitation-evaporation) signal in the closed-basin lake sediment data.

Carbonate sediment can either be clastic or authigenic (or a mixture of both), which is important since clastic carbonate is effectively a contaminant that does not reflect paleo-lacustrine environmental conditions. Formation of authigenic carbonate sediment is controlled by a variety of factors including Ca^{2+} and CO_3^{2-} ion concentrations, seasonal stratification, and primary production, wherein during algal blooms CO_2 is removed from the water, shifting the pH to higher values and the dissolved inorganic carbon (DIC) pool speciation to greater concentrations of CO_3^{2-} and HCO_3^-. This leads to greater ion availability for the formation of $CaCO_3$ in the water column, which archives the oxygen isotopic composition of the water at the time of

mineralization. In order for lacustrine carbonate isotope records to provide meaningful information about past hydrologic and environmental changes, the sediment must be demonstrably of authigenic origin. Simply determining that carbonates are present in the sediment (e.g. through LOI analysis) is therefore insufficient. SEM analysis can assist with the characterization of carbonate sediment grains. Typically, small, euhedral crystals that have not been significantly weathered can be assumed to be authigenic; whereas large, subhedral or anhedral grains can be assumed to be clastic. Measured sediment $\delta^{18}O$ values can also be compared with expected isotope values of carbonate minerals forming in isotopic equilibrium in water with $\delta^{18}O$ values and temperatures similar to that of the study site.

Isotope records can provide insight on changes in synoptic climate processes whether such processes operated in the past as they do today. Measurements of precipitation isotope values have been used globally to provide insight on ocean-atmosphere dynamics and precipitation sources (Bowen and Wilkinson 2002; Bowen 2008). Studies based on the analysis of authigenic carbonate sediment from lakes have been used in many locations globally to provide long-time scale perspectives on processes that affect water $\delta^{18}O$ values (Bird et al. 2011; Anderson 2011; Finkenbinder et al. 2016).

5.3 Shark Lake Hydrologic Characteristics

Shark Lake has one large outlet, receives inputs from both surface and groundwater, and therefore is a hydrologically open-basin lake. The stratification regime is likely dimictic, as are most small lakes in temperate climates that stratify due to temperature, although the shallow depth (4.3 m) may preclude bottom water anoxia and allow for wind-based mixing to the water-sediment interface during summer storms. The lake mixing regime likely did not vary significantly over the Holocene since there is no evidence of basin morphology having changed significantly (e.g. through mass movements in the catchment), although sustained drought could have led to the lake dropping below its outlet. Since Shark Lake is fed by both snowmelt and direct precipitation, the average lake temperature is likely dependent on when precipitation occurs. The local meteoric water line (LMWL) in the Kananaskis region has a slope close

to that of the global meteoric water line (GMWL), ~8, as defined by estimated monthly precipitation isotope values (Araguás-Araguás et al. 2000; Bowen and Wilkinson 2002). Shark Lake water isotope values plot along the meteoric water line near the intersection of the LEL (Figure 12), indicating that precipitation isotope values, which are modified by atmospheric temperature and seasonality changes, are the principal control on water isotope ratios.

5.4 Sediment Lithology

Lithological analysis of sediment cores is important for identifying facies changes indicative of shifts in various lake/catchment conditions (Rowan et al. 1992). Bulk sediment properties such as texture, organic matter content, and fossil presence (diatoms, mollusks) can provide information on productivity and lake-level changes. Bulk sediment composition can be determined by loss-on-ignition, which determines percentages of organic matter, carbonate, and residual mineral matter. Clastic sediments such as tephra or glacial deposits generally have relatively high concentrations of silicate minerals. XRF can help identify elements that are associated with clastic deposition such as titanium, iron, and silicon (Shapley et al. 2009). We characterized bulk sediment texture through XRD and SEM analysis to ensure that the carbonate sediment in Shark Lake is authigenic (Figure 8, Figure 9).

5.5 Shark Lake Multi-Proxy Record Discussion

Most of the Shark Lake $\delta^{18}O$ values are within the range of expected values based on theoretical equilibrium fractionation between water and calcite. Values from near the clay transition at the base of sequence are the most positive of the record likely as a result of the presence of clastic carbonate minerals which would bias the results toward more positive values (Figure 13). Likewise, the pronounced increase in $\delta^{18}O$ in the past century is potentially a result of catchment erosion associated with logging or other land cover changes. It is likely that the lake temperature does not vary much seasonally due to the low residence time of the lake and extensive groundwater inputs, and consequently that the influence of calcification temperature changes on sediment $\delta^{18}O$ values it minimal. Collectively, these results indicate that $\delta^{18}O$ values of the authigenic carbonate sediment

in Shark Lake are an effective proxy for reconstructing past changes in precipitation isotope values.

The Shark Lake sediment record has a two relatively linear sedimentation rates, split between below the Mazama tephra and above, with the latter being about twice as high. The sediment density gradually increases down-core, with relatively high values below the Mazama tephra, where the average density is ~0.50 g/cm^3, in comparison with ~0.35 g/cm^3 above the Mazama tephra (and below 30 cm from the surface). Ash from the Mazama eruption was focused by erosion in the Shark Lake catchment, leading to the deposition of ~75 cm of consolidated tephra that increased the density of the sediment below. However, the total sediment flux also increased after the Mazama tephra deposition (Figure 7). The Mazama tephra influenced the sediment flux by likely shifting clastic sediment provenance from weathering of glacially deposited boulders and a thin layer of rock flour to a plentiful amount of tephra. The tephra could have also led to more nutrient availability and substrate for terrestrial plants, which leads to more nutrients, like nitrogen, being fixed by terrestrial plans and subsequently running off into Shark Lake. The organic matter preserved in the Shark Lake core reflects more productivity after the tephra deposition.

The majority of the sediment record is fine carbonate mud, and the age model indicates there are not any large unconformities in the record. Although there are several interceding clastic mineral layers, sediment deposition rates, LOI results, and SEM images support that carbonate sediment has continuously accumulated since the lake initially formed as a result of authigenic production. There are several sediment layers that interrupt the generally continuous carbonate sediment classified as Unit A in the Shark Lake sequence. These layers indicate that the depositional environment of the lake varied to an extent significant enough, albeit for relatively short time periods, to produce identifiable changes in the core lithology. A minerogenic layer at 139 cm in the core, which dates to 4,900 yr BP, demonstrates that catchment erosion rates increased, perhaps in response to fresh surface exposures associated with mass wasting, that led to about 1 cm of clastic deposition. A decline in $\delta^{18}O$ values at this time indicates that increased winter precipitation may have led to greater catchment erosion and clastic deposition.

The $\delta^{18}O$ record from the Oregon Caves National Monument (OCNM) speleothem exhibits a similar decrease around that time, despite the generally increasing trend in the record overall during this interval (Ersek et al. 2012). This layer may also have resulted from lower lake levels, although the duration of the low stand must have been short given that there is no indication of a disconformity in the age model. There is evidence from dendroclimatology that historical records from the Canadian Rockies do not capture the extent of extreme droughts in the Holocene. Such clastic layers provide support for this inference, suggesting that extreme events are possible and that they may be discernable in lacustrine sediment records. (Ault et al. 2014; Sauchyn et al. 2003; Sauchyn et al. 2015).

The basal age of the Shark Lake record is ~11,000 yr BP; however the $\delta^{18}O$ data from this time are not useful for hydroclimate reconstruction due to possible clastic carbonate contamination derived from the erosion of calcareous glacial till in the catchment and subsequent deposition in the lake. The $\delta^{18}O$ record exhibits a decreasing trend from 10,000 yr BP to ~7,900, which indicates a shift toward greater cold season precipitation and/or a reduction in warm season precipitation. This part of the record has a lower temporal resolution as well due to a slower sedimentation rate and thus does not provide information at as high a temporal resolution as younger sections of the record.

At ~7,500 yr BP, $\delta^{18}O$ values exhibit a marked increase and then decrease for ~300 years, remaining low between ~7,200 and 6,400 yr BP, changes that may be related to the deposition of the Mazama tephra, its subsequent weathering and erosion, and consequent effects on lake level and water chemistry (Steinman et al. 2019). XRF analysis indicates an increase in both calcium and sulfur directly after the Mazama tephra deposition that could be indicative of an extreme lake low stand if gypsum was deposited as an evaporite mineral. Large increases in $\delta^{18}O$ around 6,500 and 6,000 yr BP mark a period of sustained higher values until a decrease at ~5,300 yr BP, which is coincident with a clastic layer at 137 cm. From 5,300 to 3,500 yr BP there are several century timescale changes in $\delta^{18}O$, with pronounced multidecadal, high amplitude variability centered on ~4,500 yr BP. A large negative excursion in $\delta^{18}O$ occurs at 4,300 yr BP and is the lowest $\delta^{18}O$ value other than at 6,700 yr BP. There is a general increasing trend in $\delta^{18}O$ from the mid-Holocene into the late Holocene, which may indicate a shift to either

less cold season precipitation or greater warm season precipitation, or some combination of the two. Overall, more negative $\delta^{18}O$ values occur in the Shark Lake record during the mid-Holocene from about 7,500 to 3,500 yr BP relative to the late Holocene after 3,500 yr BP.

Shark Lake $\delta^{18}O$ values increase through the late Holocene, a trend that is overlain by progressively increasing short-term, multi-decadal climate variability. The steady increase from 3,500 to 1,700 yr BP indicates a shift toward a greater warm season precipitation contribution to annual totals. Low values in the $\delta^{18}O$ data around 600 yr BP may correlate with expansion of alpine glaciers in the Canadian Rocky Mountains during the Little Ice Age. Century to decadal scale variations and increasing $\delta^{18}O$ values in the Late Holocene suggest that modern ENSO dynamics were becoming established (Steinman et al. 2016), which influenced the expression of the PNA after the end of the Little Ice Age. $\delta^{18}O$ values increase markedly at this time, which indicates either a further shift in precipitation seasonality toward a greater warm season component and a possible loss of winter snowpack (Anderson 2011) and/or the influence of clastic contamination introduced by catchment destabilization associated land cover change.

The sediment at the top of the sequence, from around 100 yr BP to present, is unconsolidated and contains carbonates with higher $\delta^{18}O$ values than elsewhere in the record (other than the lowermost section of the core). These high values may in part be related the upward trend in $\delta^{18}O$ that occurs throughout the late Holocene, but the shift in the rate of change of $\delta^{18}O$ increase is most likely a result of either a hydrologic change or catchment destabilization and a consequent increase in clastic carbonate relative to authigenic carbonate deposition. The $\delta^{18}O$ record from Bison Lake, CO, exhibits a similar increase in modern sediments that is asserted to have resulted from both climate variation, an increase in winter precipitation, and the impoundment of the lake in 1950 (Anderson 2011). There is no clear evidence of human influence on the Shark Lake catchment substantial enough to affect the hydrology, but it is possible that logging occurred at some point in the recent past. If clear cutting occurred in the Shark Lake catchment, it likely would have had a substantial hydrological effect on the landscape through impacts on soil depth, evapotranspiration rates and runoff. Previous studies in the

Kananaskis Valley demonstrated increased catchment runoff after modern logging; although suspended sediment in streams did not increase. These studies suggest that the carbonate substrate was stable and the watershed resilient to land cover and hydrologic changes (Harder et al. 2015; Swanson et al. 1986). Extrapolation of the conclusions of these studies is difficult given that catchment slope, vegetation composition, and soil/sediment characteristics are highly variable in mountainous settings. Early logging records are either incomplete or unavailable, so the timing and spatial patterns of early logging and the consequent catchment denudation are not well known.

5.6 Regional Sediment Core Lithology

Sediment cores from Lower Burstall Lake, about 8 km southeast Shark Lake indicate the establishment of a post-glacial landscape with extensive clastic clay deposits and shrub pollen near the base of the sediment sequence, dated to greater than 10,000 yr BP (Beierle et al. 2003). This is consistent with the clastic carbonate-rich clay at the bottom of the Shark Lake record, which marked a cold period as the Canmore Advance receded and clastic sediment was eroded from the landscape (Bobrowsky and Rutter 1992). The basal sediment from Wedge Lake, ~18 kilometers east of Shark Lake in the adjacent valley and at about 1,500 m ASL, contains abundant clay and dates to 10,400 yr BP. Yamnuska Bog near Morely Flats, AB, (MacDonald 1982) also contains clay-rich clastic sediment in the lowermost section of the sequence. Unit D in the Shark Lake sequence has an age greater that 10,500 yr BP and is likely of glacial origin, consistent with other local lacustrine sediment records (Table 1, Figure 11).

Yamnuska Bog, Wedge Lake, and Burstall Lake all contain carbonate sediments. The record from Lower Burstall Lake contains a carbonate-rich mud layer (referred to as marl by the authors) that dates to 9,180±60 ^{14}C yr BP or 10,200 yr BP on the basis of one ^{14}C age point from the center of the layer (Beierle et al. 2003). In the Lower Burstall sequence, organic-rich sediment occurs both above and below the Mazama tephra with a transition upward to greater carbonate content; however this is considered clay by the authors (Beierle et al. 2003). The carbonate-rich sediment could be authigenic but it is not specified as such. The sequence in textural changes from clay to authigenic carbonate to organic sediment (referred to as gyttje in Beierle et al. 2003) in the Burstall Lake record

indicates a warming trend from 10,000 to 7,000 yr BP. The occurrence of clastic sediment is interpreted as a reconnection to a sediment source such as glacial outwash plains and/or less vegetation in the catchment during Neoglacial period re-advance from 3,500 to present (Beierle et al. 2003). In the Wedge Lake record, textural changes below the Mazama tephra are abrupt where deposition transitioned from clay to silt with a larger grain size and lower carbonate content. Yamnuska Bog has a similar sequence to that of Lower Burstall Lake, although the carbonate sediment was deposited after glacial clays accumulated at ~1,140±70 ^{14}C yr BP, In the Yamnuska Bog record the carbonate sediment is overlain by peat. Wedge Lake and Yamnuska Bog records are thought to not be as sensitive to sediment type changes as Lower Burstall Lake but rather to indicate differences in lake responses in the mountains versus the foothills.

5.7 δ^{18}O Record Comparison

The inferred changes to precipitation amount and seasonality during the mid- to late Holocene in western North America are spatially variable and at least to some extent inconsistent across records (Shuman et al. 2018; Liu et al. 2014). In order to be useful for investigating the influence of multi-decadal synoptic climate oscillations, lacustrine paleoproxy records must have sufficient temporal resolution (e.g. at least decadal) data with age control sufficient to ensure that the data are continuous and that sedimentation rates do not vary substantially. Records that capture precipitation seasonality and isotope values are important for reconstructing changes in PNA-like atmospheric circulation in the topographically complex regions of western North America (Anderson 2011; Sauchyn et al. 2015). The Shark Lake record tracks precipitation seasonality changes in response Pacific ocean-atmosphere dynamics.

Variability the Shark Lake δ^{18}O record is in part controlled by water temperature as well as catchment processes that affect sedimentation and hydrology. For example, depleted δ^{18}O values during the mid-Holocene in the Shark Lake record could be seen as having resulted from the influence of water temperature on the calcite-water isotopic fractionation, which modifies δ^{18}O ratios by ~0.24 ‰/°C (Kim and O'Neil 1997). The Oregon Caves National Monument (OCNM) speleothem δ^{18}O record has a high temporal resolution (exceeding that of Shark Lake), covers the same time period as the Shark Lake

sediment (with the exception of a hiatus between 8,000-9,500 yr BP) and provides a reconstruction of past changes in precipitation isotope values in the absence of changes in water temperature at the location of calcite formation (Ersek et al. 2012). Cave deposits form in temperature-controlled environments relative to lakes, due to their underground locations, and the hydrology of the OCNM cave system is controlled by precipitation infiltration and groundwater flow into the cave. Both the OCNM and Shark Lake $\delta^{18}O$ records exhibit variability associated with changes in precipitation seasonality and are similar ($r=0.45$ $P=0.02$), demonstrating that Shark Lake is strongly influenced by Pacific Ocean SST and atmospheric teleconnections more so than lake water temperature changes (Ersek et al. 2012) (Figure 14, Table 2). The OCNM record has a significant positive correlation ($p < 0.1$) to the Shark Lake record at filtering frequencies ranging from 10 to 500 years (Table 2).

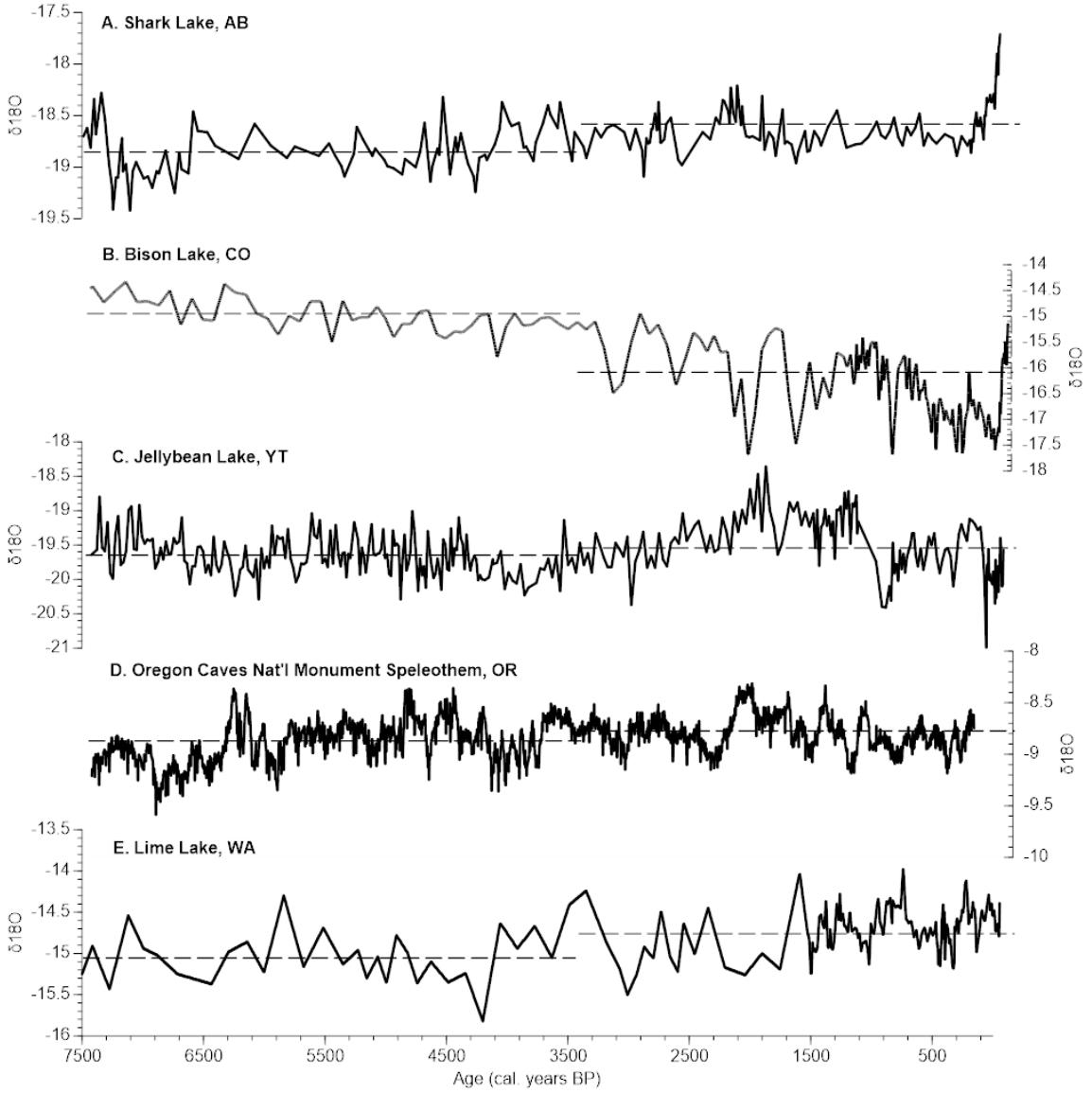

Figure 14 – Western North America lake sediment and speleothem record comparison

A comparison of records from lake and speleothem $\delta^{18}O$ records.

A. Shark Lake, AB
B. Bison Lake, CO (Anderson, 2012)
C. Jellybean Lake, YT (Anderson et al., 2016)
D. OCNM, OR speleothem (Ersek et al., 2012)
E. Lime Lake, WA (Steinman et al., 2016)

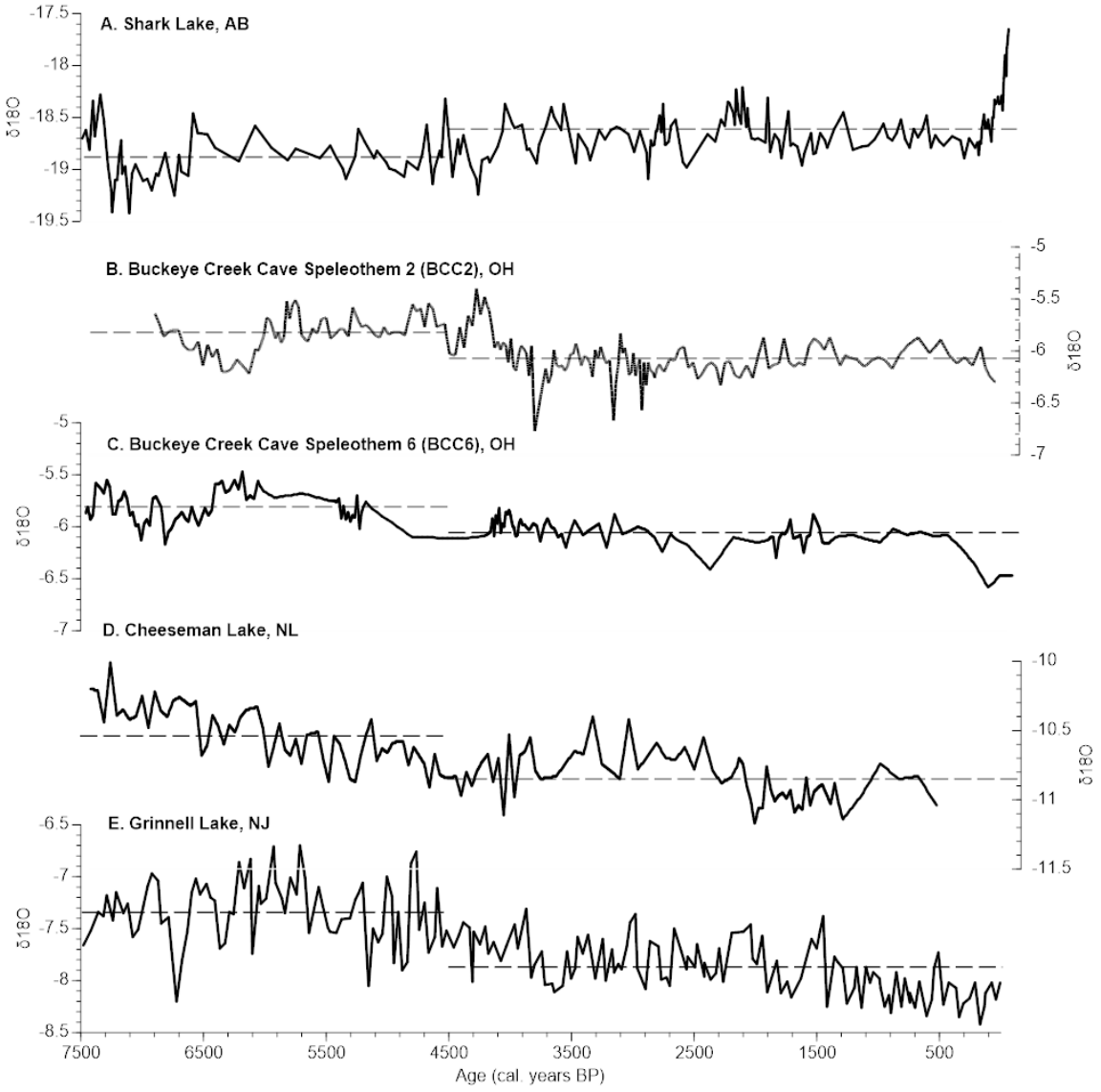

Figure 15 – Northeast North America lake sediment and speleothem record comparison

A comparison of records from lake and speleothem $\delta^{18}O$ records.

A. Shark Lake, AB
B. Buckeye Creek Cave Speleothem 2 (BCC2), OH (Hardt et al, 2010)
C. Buckeye Creek Cave Speleothem 6 (BCC6), OH (Hardt et al, 2010)
D. Cheeseman Lake, NL (Finkenbinder et al., 2016)
E. Grinnell Lake, NJ (Zhao et al., 2010)

Filter Frequency None	Range	Jellybean	OCNM	Lime	Bison	BCC2	BCC6	Cheeseman	Grinnell
p	0.02	0.00	0.00	0.00	0.00	0.00	0.00	0.00	0.00
	0.16	0.02	0.00	0.00	0.00	0.00	0.00	0.00	0.00
	0.50	0.17	0.00	0.00	0.00	0.00	0.00	0.00	0.00
	0.84	0.60	0.00	0.01	0.00	0.00	0.01	0.00	0.00
	0.98	0.94	0.02	0.03	0.01	0.01	0.06	0.01	0.02
r	0.02	-0.08	0.20	0.18	-0.46	-0.44	-0.39	-0.45	-0.42
	0.16	0.03	0.28	0.24	-0.41	-0.39	-0.34	-0.39	-0.38
	0.50	0.11	0.34	0.29	-0.35	-0.34	-0.28	-0.34	-0.34
	0.84	0.19	0.40	0.34	-0.30	-0.29	-0.23	-0.28	-0.29
	0.98	0.26	0.45	0.40	-0.24	-0.22	-0.17	-0.21	-0.24
10 yr									
p	0.02	0.00	0.00	0.00	0.00	0.00	0.00	0.00	0.00
	0.16	0.02	0.00	0.00	0.00	0.00	0.00	0.00	0.00
	0.50	0.17	0.00	0.00	0.00	0.00	0.00	0.00	0.00
	0.84	0.60	0.00	0.01	0.00	0.00	0.01	0.00	0.00
	0.98	0.94	0.02	0.03	0.01	0.01	0.06	0.01	0.02
r	0.02	-0.08	0.20	0.18	-0.46	-0.44	-0.39	-0.45	-0.42
	0.16	0.03	0.28	0.24	-0.41	-0.39	-0.34	-0.39	-0.38
	0.50	0.11	0.34	0.29	-0.35	-0.34	-0.28	-0.34	-0.34
	0.84	0.19	0.40	0.34	-0.30	-0.29	-0.23	-0.28	-0.29
	0.98	0.26	0.45	0.40	-0.24	-0.22	-0.17	-0.21	-0.24
50 yr									
p	0.02	0.00	0.00	0.00	0.00	0.00	0.00	0.00	0.00
	0.16	0.00	0.00	0.00	0.00	0.00	0.00	0.00	0.00
	0.50	0.03	0.00	0.00	0.00	0.00	0.00	0.00	0.00
	0.84	0.40	0.00	0.00	0.00	0.00	0.00	0.00	0.00
	0.98	0.89	0.00	0.00	0.00	0.00	0.00	0.00	0.00
r	0.02	-0.09	0.22	0.19	-0.49	-0.49	-0.43	-0.49	-0.45
	0.16	0.03	0.31	0.26	-0.44	-0.44	-0.37	-0.43	-0.40
	0.50	0.12	0.37	0.31	-0.38	-0.38	-0.31	-0.37	-0.36
	0.84	0.20	0.44	0.37	-0.32	-0.32	-0.25	-0.31	-0.31
	0.98	0.28	0.49	0.43	-0.26	-0.25	-0.18	-0.23	-0.25
100 yr									
p	0.02	0.00	0.00	0.00	0.00	0.00	0.00	0.00	0.00
	0.16	0.00	0.00	0.00	0.00	0.00	0.00	0.00	0.00
	0.50	0.08	0.00	0.00	0.00	0.00	0.00	0.00	0.00
	0.84	0.54	0.00	0.00	0.00	0.00	0.00	0.00	0.00
	0.98	0.89	0.00	0.01	0.00	0.00	0.01	0.00	0.00
r	0.02	-0.11	0.24	0.21	-0.52	-0.53	-0.46	-0.52	-0.48
	0.16	0.03	0.34	0.28	-0.46	-0.48	-0.39	-0.45	-0.43
	0.50	0.13	0.41	0.34	-0.40	-0.42	-0.33	-0.40	-0.39
	0.84	0.23	0.48	0.40	-0.34	-0.35	-0.27	-0.33	-0.33
	0.98	0.31	0.53	0.47	-0.27	-0.28	-0.20	-0.25	-0.27
500 yr									
p	0.02	0.02	0.00	0.00	0.00	0.00	0.00	0.00	0.00
	0.16	0.09	0.00	0.00	0.00	0.00	0.00	0.00	0.00
	0.50	0.31	0.00	0.00	0.00	0.00	0.01	0.00	0.00
	0.84	0.69	0.01	0.02	0.01	0.00	0.04	0.01	0.00
	0.98	0.96	0.05	0.05	0.03	0.02	0.12	0.06	0.02
r	0.02	-0.11	0.36	0.34	-0.67	-0.72	-0.59	-0.66	-0.66
	0.16	0.04	0.48	0.42	-0.60	-0.66	-0.52	-0.59	-0.61
	0.50	0.18	0.58	0.50	-0.53	-0.60	-0.45	-0.52	-0.56
	0.84	0.31	0.66	0.56	-0.46	-0.52	-0.37	-0.45	-0.50
	0.98	0.41	0.73	0.63	-0.37	-0.43	-0.28	-0.34	-0.42

Table 2 – Statistical comparison of the Shark Lake record to other oxygen isotope records

Correlations (r) and significance (p) values for each pair of records are based on 1000 realizations of the age model of each record. The one and two σ and median values from each correlation distribution are presented (denoted in the range column as 0.02 - two σ low, 0.16 - one σ low, 0.50 - median, 0.84 - one σ high, and 0.98 - two σ high). A p value of less than 0.1 at the two σ high.

The Lime Lake, WA, $\delta^{18}O$ record, another open-basin carbonate sediment dataset, exhibits a long-term trend that is highly similar (r=0.4, p=0.01,100 yr filter) to that of Shark Lake (Table 2) (Steinman et al. 2016). The Shark and Lime Lake records are strongly correlated over most low pass filter periods, which shows that both long and short term climate changed similarly in eastern Washington and the Southern Canadian Rockies (Table 2). However, a few differences occur in the $\delta^{18}O$ records, for example, in the last 200 years of the record where the Shark Lake $\delta^{18}O$ values increase in contrast to $\delta^{18}O$ values in Lime Lake, which do so at a much lower rate. This observation provides additional evidence that the Shark Lake $\delta^{18}O$ record may have been affected by clastic contamination in the surface sediment. The Lime Lake record also exhibits a more pronounced decreasing trend from 5,700 to 4,300 yr BP, which may indicate that the Cascade-Rocky Mountain intermontane setting of Lime Lake could have been more strongly influenced by Pacific ocean-atmosphere variability changes due perhaps to its closer proximity and/or controls associated with orography. (Table 2).

An open-basin lake $\delta^{18}O$ record from Bison Lake, CO, located in the Southern Rocky Mountains has a Holocene pattern that is opposite those of Shark Lake, Lime Lake, and the OCNM speleothem, suggesting substantially different responses in precipitation isotope values to changes in Pacific ocean-atmosphere dynamics (Anderson 2011; Anderson 2012; Anderson et al. 2016, Table 2). The Bison Lake record has a strong negative correlation to the Shark Lake record (r=-0.24, p=0.01), which is consistent with the modern PNA precipitation isotope pattern (Liu et al. 2014). Furthermore, $\delta^{18}O$ records from open basin lakes located in eastern North America including Cheeseman Lake (NL) and Grinnell Lake (NJ) and the Buckeye Creek Cave (BCC) speleothem series from West Virginia, also exhibit Holocene trends opposite that of Shark Lake (Finkenbinder et al. 2016; Hardt et al. 2010) (Figure 15). These records are all negatively correlated with the Shark Lake isotope record across a range of filter frequencies (Table 2) indicating that low frequency variability in the climate system is likely driving shifts in the precipitation isotope values on a continent wide scale in response to changes in Pacific basin ocean-atmosphere dynamics.

Jellybean Lake in the Yukon Territories, Canada is much like the Bison Lake record in the mid-Holocene with a decreasing trend from 7,500 to 6,300 yr BP. Jellybean Lake is strongly influenced by the strength and position of the Aleutian Low (AL) which is controlled by PDO/ENSO variability (Anderson et al. 2016; Rodionov, Bond, and Overland 2007). The Jellybean record is not significantly correlated to the Shark Lake record ($r=0.26$, $p=0.94$). The Jellybean record exhibits different trends likely due to changes in the AL versus the PNA control in the other records. The Jellybean record has more enriched $\delta^{18}O$ values in the late Holocene compared to the mid-Holocene which is the inverse of the Shark Lake record.

The Shark Lake $\delta^{18}O$ record is consistent with the pattern of Holocene precipitation isotope changes identified by Liu et al. 2014 and hypothesized to be related to a shift in PNA-like mean state conditions at ~4,000 yr BP. Notably, the Liu et al. 2014 study analyzed only four records (Jellybean, OCNM, BCC, and Grinnell) to make assertions regarding broad scale climate change across North America; whereas here we present recently published data from Lime Lake, Bison Lake, Cheeseman Lake, and the newly developed dataset from Shark Lake. Consistency between the Shark Lake $\delta^{18}O$ record and those from the Pacific Northwest (with the exception of Jellybean) provides further support for the Liu et al. 2014 hypothesis that a mean state shift from negative PNA-like conditions to positive PNA-like conditions occurred during the middle Holocene. The spatial differences in hydroclimate related PNA-like mean states across North America are due atmospheric pressure anomalies that affect the jet stream. A positive PNA leads to warmer conditions with more winter precipitation for the Pacific Northwest (and Shark Lake) but colder and drier winter conditions for central and eastern North America. The opposite is true during the negative phase of the PNA. Temporal changes in PNA-like mean state conditions likely caused winter precipitation changes across North America over the Holocene.

Mountain hydroclimate is highly affected by orographic effects. Small spatial scale changes can produce large differences in climate. For instance, precipitation records from high altitude regions in most of the Central and Southern Rockies are similar to those of Bison Lake; however historic records and models show areas around

Yellowstone National Park, WY/MT have an opposite trend, similar to the Northern Rocky Mountains, wherein positive precipitation to evaporation during NAM phases (Anderson et al. 2016; Steinman et al. 2016). Large spatial scale differences are also due to PNA state, with a positive PNA state producing strong meridional atmospheric flow, and a negative PNA phase leading to more zonal flow (Anderson et al. 2016). This phase change is reflected with a shift in the distribution of precipitation oxygen isotope values to more enriched during positive PNA phases due to more summer precipitation.

The PNA is also tied to multi-annual climate oscillations such as ENSO/NAM. During positive ENSO phases, the Northern Rockies have a negative precipitation to evaporation balance response (drier conditions), while the Southern Rockies have a positive response (wetter conditions) and vice versa. Shifts in stable states from ENSO and NAM are expressed as atmospheric pressure changes in the Pacific; this can influence the jet stream which leads to changes in storm tracks and seasonal moisture changes. ENSO has about a three to seven-year cycle but the data we are working with is century or decadal-scale so it tracks trends in ENSO as expressed through the multi-decadal component of the PDO and its influence on the PNA. The increasing trend in average $\delta^{18}O$ values from the mid- to late Holocene in the Shark Lake record suggests the establishment of modern ocean-atmosphere dynamics.

6. Future Work

Several questions arise from assessment of the Shark $\delta^{18}O$ record. For example, the $\delta^{18}O$ values from the base of the sediment sequence are much higher than would be expected given that climate was cold during the early Holocene deglacial phase in southern AB (Figure 13) (Beierle et al. 2003). In this section of the record, there is likely clastic carbonate contamination derived from the fine, glacial sediment that we identified as Unit D, which occurs directly beneath this interval. A similar (although opposite) pattern occurs in the surface sediment near the top of the sequence, and this indicates possible clastic contamination related to catchment destabilization. Future work could address the reasons for the high $\delta^{18}O$ values through more extensive SEM imagery of sediment from these depths in order to check for the presence of clastic carbonates. Samples from these depths could also be analyzed using XRD to compare with results

from Unit A, which indicate a minimal presence of minerals such quartz and dolomite typically associated with clastic sediment (Figure 8). The timing of catchment destabilization could be constrained through an analysis of historical logging records. Finally, isotope ratios of bedrock should be measured to quantify the potential effects of clastic contamination that could be present in the record.

The temporal resolution of the $\delta^{18}O$ record could be increased through additional analyses. Additional samples from the mid-Holocene section of the record should be measured in order to match the temporal resolution of the late-Holocene part of the record. This would help address the lack of data from several intervals, such as the potential warm period around the time of the Mazama tephra deposition, which is being studied through the development of records from comparable settings in the Pacific Northwest (Steinman et al. 2019). The transition after the Mazama tephra can also be explored more from the Shark Lake sediment composition. The XRF data reflects an increase in sulfur, which could be due to gypsum deposition (Figure 10). Gypsum is only deposited as an evaporite mineral and thus could indicate an extreme lake low-stand. XRD analysis on samples directly above the Mazama tephra would clarify this.

Another task that would strengthen the interpretation of the Shark Lake $\delta^{18}O$ record is monthly lake temperature and water chemistry monitoring. Given that lake water temperature changes in part control authigenic carbonate mineral $\delta^{18}O$ values, these data would provide insight on the extent of the influence of timing of carbonate mineral formation in the water column (i.e. time of year as it relates to temperature changes) and also the relationship between atmospheric temperature and lake water temperature on both intra-annual and inter-annual scales. Here we assumed that average lake water temperature is the same at the time of authigenic sediment formation, given that the lake is meltwater fed, and has a short residence time that disallows substantial atmospheric heating the lake, but it is possible that shifts in the timing of precipitation (e.g. from colder to warmer months or vice versa) could affect the lake water temperature.

7. Conclusions

Shark Lake has an open-basin hydrologic configuration, and the isotope values of the lake surface water are consistent with meteoric water inflows and the local meteoric water line. The authigenic carbonate sediment captures water oxygen isotope ratios during the time of carbonate mineralization, as evidenced by consistency between measured sediment $\delta^{18}O$ values and theoretical values determined using measurements of lake water $\delta^{18}O$ and an assumed temperature range. Given the large disparity (11.8 ‰ difference) between warm and cold season precipitation $\delta^{18}O$, shifts in sediment oxygen isotope values of Shark Lake therefore reflect changes in the amount and distribution of precipitation throughout the year, with lower values reflecting greater cold season precipitation (and/or less warm season precipitation) and vice versa for higher values. The Shark Lake sediment age model demonstrates continuous deposition and preservation with no unconformities. Results from LOI, XRD, and XRF indicate that the majority of the sediment sequence consists of authigenic carbonate mud with minimal clastic input, with the exception of the Mazama tephra and one layer that likely contains abundant clastic material. Collectively these data demonstrate that the Shark Lake sediment $\delta^{18}O$ record is a reliable decade to century-scale reconstruction of the isotopic composition of precipitation over the past 10,000 years.

The Shark Lake $\delta^{18}O$ record has a positive, significant correlation with other similar records from the Pacific Northwest, specifically those from Lime Lake (WA) and the OCNM (OR) speleothem (Steinman et al. 2016; Ersek et al. 2012), and has a negative, significant correlation with records from the southern Rocky Mountains and eastern North America, namely those from Bison Lake (CO), Cheeseman Lake (NL), Grinnell Lake (NJ), and the Buckeye Creek Cave speleothems (WV) (Anderson 2012; Finkenbinder et al. 2016; Zhao et al. 2010; Hardt et al. 2010). The Jellybean Lake (YT) $\delta^{18}O$ record is not significantly correlated to the Shark Lake record (Anderson et al. 2005), likely due to disparate responses to PNA-like variability in the far northern regions of the Pacific Northwest relative to the central location of Shark lake. The transition from more negative to more positive values in the Shark Lake record from the middle through the late Holocene shows that the southern Canadian Rockies experienced a decrease in

cold season precipitation (relative to warm season precipitation) during this time that is consistent with changes in PNA-like mean state variability that occurred elsewhere in North America.

The Shark Lake $\delta^{18}O$ record is a substantial contribution to the growing body of research on Holocene paleoclimate in western North America, and is particularly important because records of precipitation isotope variability are relatively uncommon but critical for both assessing changes in precipitation seasonality and providing baseline precipitation isotope data that can be used to isolate the precipitation-evaporation balance signal from closed-basin lake $\delta^{18}O$ records (Steinman et al. 2016). This research will provide a long-term perspective on hydroclimate in the Canadian Great Plains, a region where water resources are critical for the expanding population and industry. Long term proxies of precipitation and droughts can identify trends that have not been observed during the historical period and can provide water resource managers with a more throughout understanding the timing and magnitude of potential changes in future hydroclimate.

8. Bibliography

Abbott, Mark B., and Thomas W. Stafford. 1996. “Radiocarbon Geochemistry of Modern and Ancient Arctic Lake Systems, Baffin Island, Canada.” *Quaternary Research* 45 (3): 300–311. doi:10.1006/qres.1996.0031.

Anderson, Lesleigh. 2011. “Holocene Record of Precipitation Seasonality from Lake Calcite Δ18O in the Central Rocky Mountains, United States.” *Geology* 39 (3): 211–14. doi:10.1130/G31575.1.

———. 2012. “Rocky Mountain Hydroclimate: Holocene Variability and the Role of Insolation, ENSO, and the North American Monsoon.” *Global and Planetary Change* 92–93. Elsevier B.V.: 198–208. doi:10.1016/j.gloplacha.2012.05.012.

Anderson, Lesleigh, Mark B. Abbott, Bruce P. Finney, and Stephen J. Burns. 2005. “Regional Atmospheric Circulation Change in the North Pacific during the Holocene Inferred from Lacustrine Carbonate Oxygen Isotopes, Yukon Territory, Canada.” *Quaternary Research* 64 (1): 21–35. doi:10.1016/j.yqres.2005.03.005.

Anderson, Lesleigh, Max Berkelhammer, John A. Barron, Byron A. Steinman, Bruce P. Finney, and Mark B. Abbott. 2016. “Lake Oxygen Isotopes as Recorders of North American Rocky Mountain Hydroclimate: Holocene Patterns and Variability at Multi-Decadal to Millennial Time Scales.” *Global and Planetary Change* 137. Elsevier B.V.: 131–48. doi:10.1016/j.gloplacha.2015.12.021.

Anderson, Lesleigh, Andrea Brunelle, and Robert Thompson. 2015. “A Multi-Proxy Record of Hydroclimate, Vegetation, Fire, and Post-Settlement Impacts for a Subalpine Plateau, Central Rocky Mountains, U.S.A.” *Holocene* 25 (6): 932–43. doi:10.1177/0959683615574583.

Appleby, P. G., and F. Oldfield. 1983. “The Assessment of ^{210}Pb Data from Sites with Varying Sediment Accumulation Rates.” *Hydrobiologia* 103 (1): 29–35. doi:10.1007/BF00028424.

Araguás-Araguás, L., K. Froehlich, and K. Rozanski. 2000. “Deuterium and Oxygen-18 Isotope Composition of Precipitation and Atmospheric Moisture.” *Hydrological Processes* 14 (8): 1341–55. doi:10.1002/1099-1085(20000615)14:8<1341::AID-HYP983>3.0.CO;2-Z.

Asmerom, Yemane, Victor Polyak, Stephen Burns, and Jessica Rassmssen. 2007. “Solar Forcing of Holocene Climate: New Insights from a Speleothem Record, Southwestern United States.” *Geology* 35 (1): 1–4. doi:10.1130/G22865A.1.

Ault, Toby R., Julia E. Cole, Jonathan T. Overpeck, Gregory T. Pederson, and David M. Meko. 2014. “Assessing the Risk of Persistent Drought Using Climate Model Simulations and Paleoclimate Data.” *Journal of Climate* 27 (20): 7529–49. doi:10.1175/JCLI-D-12-00282.1.

Barron, John A., and Lesleigh Anderson. 2011. “Enhanced Late Holocene ENSO/PDO Expression along the Margins of the Eastern North Pacific.” *Quaternary International* 235 (1–2). Elsevier Ltd: 3–12. doi:10.1016/j.quaint.2010.02.026.

Beierle, Brandon D., Derald G. Smith, and Leonard V. Hills. 2003. “Late Quaternary

Glacial and Environmental History of the Burstall Pass Area, Kananaskis Country, Alberta, Canada." *Arctic, Antarctic, and Alpine Research* 35 (3): 391–98. doi:10.1657/1523-0430(2003)035[0391:LQGAEH]2.0.CO;2.

Bird, Broxton W., Mark B. Abbott, Donald T. Rodbell, and Mathias Vuille. 2011. "Holocene Tropical South American Hydroclimate Revealed from a Decadally Resolved Lake Sediment Δ18O Record." *Earth and Planetary Science Letters* 310 (3–4). Elsevier B.V.: 192–202. doi:10.1016/j.epsl.2011.08.040.

Bird, Broxton W., Pratigya J. Polisar, Yanbin Lei, Lonnie G. Thompson, Tandong Yao, Bruce P. Finney, Daniel J. Bain, David P. Pompeani, and Byron A. Steinman. 2014. "A Tibetan Lake Sediment Record of Holocene Indian Summer Monsoon Variability." *Earth and Planetary Science Letters* 399. Elsevier B.V.: 92–102. doi:10.1016/j.epsl.2014.05.017.

Bird, Broxton W., Jeremy J. Wilson, William P. Gilhooly, Byron A. Steinman, and Lucas Stamps. 2017. "Midcontinental Native American Population Dynamics and Late Holocene Hydroclimate Extremes." *Scientific Reports* 7 (317): 1–13. doi:10.1038/srep41628.

Bird, Broxton W, Mark B Abbott, Mathias Vuille, Donald T Rodbell, Nathan D Stansell, and Michael F Rosenmeier. 2011. "A 2,300-Year-Long Annually Resolved Record of the South American Summer Monsoon from the Peruvian Andes." *Proceedings of the National Academy of Sciences of the United States of America* 108 (21): 8583–88. doi:10.1073/pnas.1003719108.

Bobrowsky, Peter, and Nathaniel W. Rutter. 1992. "The Quaternary Geologic History of the Canadian Rocky Mountains." *Géographie Physique et Quaternaire* 46 (1): 5. doi:10.7202/032887ar.

Bowen, Gabriel J. 2008. "Spatial Analysis of the Intra-Annual Variation of Precipitation Isotope Ratios and Its Climatological Corollaries." *Journal of Geophysical Research Atmospheres* 113 (5): 1–10. doi:10.1029/2007JD009295.

Bowen, Gabriel J., and Justin Revenaugh. 2003. "Interpolating the Isotopic Composition of Modern Meteoric Precipitation." *Water Resources Research* 39 (10): 1–13. doi:10.1029/2003WR002086.

Bowen, Gabriel J, and Bruce Wilkinson. 2002. "Spatial Distribution Δ18O Meteoric Precipitation." *Geology* 30 (4): 315–18. doi:10.1130/0091-7613(2002)030<0315.

Briffa, K R, P D Jones, and F H Schweingruber. 1992. "Tree-Ring Density Reconstructions of Summer Temperature Patterns across Western North America since 1600." *Journal of Climate*. doi:10.1175/1520-0442(1992)005<0735:TRDROS>2.0.CO;2.

Dansgaard, W. 1964. "Stable Isotopes in Precipitation." *Tellus* 16 (4): 436–68. doi:10.3402/tellusa.v16i4.8993.

Davis, Margaret B., and Daniel B. Botkin. 1985. "Sensitivity of Cool-Temperate Forests and Their Fossil Pollen Record to Rapid Temperature Change." *Ecology, Evolution and Behavior* 23 (3): 327–40.

Donahue, D J, T W Linick, and A J T Jull. 1990. “Isotope-Ratio and Background Corrections for Accelerator Mass Spectrometry Ratiocarbon Measurements.” *Radiocarbon* 32 (2): 135–42. papers2://publication/uuid/46C9FE51-5E79-4FEB-945F-3D0081101FA7.

Dyke, Arthur S. 2004. “An Outline of the Deglaciation of North America with Emphasis on Central and Northern Canada.” *Quaternary Glaciations-Extent and Chronology, Part II: North America* 2b: 373-424. doi:10.1016/S1571-0866(04)80209-4.

Ersek, Vasile, Peter U. Clark, Alan C. Mix, Hai Cheng, and R. Lawrence Edwards. 2012. “Holocene Winter Climate Variability in Mid-Latitude Western North America.” *Nature Communications* 3. Nature Publishing Group: 1218–19. doi:10.1038/ncomms2222.

Evans, David J.a., Keith E. Salt, and Claire S. Allen. 1999. “Glacitectonized Lake Sediments, Barrier Lake, Kananaskis Country, Canadian Rocky Mountains.” *Canadian Journal of Earth Sciences* 36: 395–407. doi:10.1139/cjes-36-3-395.

Finkenbinder, Matthew S., Mark B. Abbott, and Byron A. Steinman. 2016. “Holocene Climate Change in Newfoundland Reconstructed Using Oxygen Isotope Analysis of Lake Sediment Cores.” *Global and Planetary Change* 143. Elsevier B.V.: 251–61. doi:10.1016/j.gloplacha.2016.06.014.

Fleming, Sean W, and David J Sauchyn. 2013. “Availability, Volatility, Stability, and Teleconnectivity Changes in Prairie Water Supply from Canadian Rocky Mountain Sources over the Last Millennium.” *Water Resources Research* 49 (1): 64–74. doi:10.1029/2012WR012831.

Gat, J. R. 1996. “Oxygen and Hydrogen Isotopes in the Hydrologic Cycle.” *Annual Review Earth Planetary Science* 24: 225–62.

Hallett, D. J., L. V. Hills, and J. J. Clague. 1997. “New Accelerator Mass Spectrometry Radiocarbon Ages for the Mazama Tephra Layer from Kootenay National Park, British Columbia, Canada.” *Canadian Journal of Earth Sciences* 34 (9): 1202–9. doi:10.1139/e17-096.

Harder, Phillip, John W Pomeroy, and Cherie J Westbrook. 2015. “Hydrological Resilience of a Canadian Rockies Headwaters Basin Subject to Changing Climate, Extreme Weather, and Forest Management.” *Hydrological Processes* 29 (18): 3905–24. doi:10.1002/hyp.10596.

Hardt, Ben, Harold D. Rowe, Gregory S. Springer, Hai Cheng, and R. Lawrence Edwards. 2010. “The Seasonality of East Central North American Precipitation Based on Three Coeval Holocene Speleothems from Southern West Virginia.” *Earth and Planetary Science Letters* 295 (3–4). Elsevier B.V.: 342–48. doi:10.1016/j.epsl.2010.04.002.

Haslett, John, and Andrew Parnell. 2008. “A Simple Monotone Process with Application to Radiocarbon-Dated Depth Chronologies.” *Journal of the Royal Statistical Society. Series C: Applied Statistics* 57 (4): 399–418. doi:10.1111/j.1467-9876.2008.00623.x.

Heiri, O, A.F. Lotter, and G. Lemcke. 2001. “Loss on Ignition as a Method for

Estimating Organic and Carbonate Content in Sediments: Reproducibility and Comparability of Results." *Journal of Paleolimnology* 25 (1): 101–10. doi:https://doi.org/10.1023/A:1008119611481.

Hodell, David A., Claire L. Schelske, Gary L. Fahnenstiel, and Lisa L. Robbins. 1998. "Biologically Induced Calcite and Its Isotopic Composition in Lake Ontario." *Limnology and Oceanography* 43 (2): 187–99. doi:10.4319/lo.1998.43.2.0187.

Hu, F, D Kaufman, S Yoneji, D Nelson, A Shemesh, Y Huang, J Tian, G Bond, B Clegg, and T Brown. 2003. "Cyclic Variation and Solar Forcing of Holocene Climate in the Alaska Subarctic." *Science* 301 (September): 1890–93.

Johnson, E.A., and G.I. Fryer. 1987. "Historical Vegetation Change in the Kananaskis Valley, Canadian Rockies." *Canadian Journal of Botany* 65 (5): 853–58. doi:10.1139/b87-116.

Johnson, E A, and G I Fryer. 1989. "Population Dynamics in Lodgepole Pine - Engelmann Spruce Forests." *Ecology* 70 (5): 1335–45. http://www.jstor.org/stable/pdfplus/1938193.pdf.

Kelts, K, and K. J. Hsü. 1978. "Lakes : Freshwater Carbonate Sedimentation." *Lakes*, 295–323. doi:10.1007/978-1-4757-1152-3_9.

Kim, Jung Hyun, Norel Rimbu, Stephan J. Lorenz, Gerrit Lohmann, Seung Il Nam, Stefan Schouten, Carsten Rühlemann, and Ralph R. Schneider. 2004. "North Pacific and North Atlantic Sea-Surface Temperature Variability during the Holocene." *Quaternary Science Reviews* 23 (20–22 SPEC. ISS.): 2141–54. doi:10.1016/j.quascirev.2004.08.010.

Kim, Sang Tae, and James R. O'Neil. 1997. "Equilibrium and Nonequilibrium Oxygen Isotope Effects in Synthetic Carbonates." *Geochimica et Cosmochimica Acta* 61 (16): 3461–75. doi:http://dx.doi.org/10.1016/S0016-7037(97)00169-5.

Kim, Sang Tae, James R. O'Neil, Claude Hillaire-Marcel, and Alfonso Mucci. 2007. "Oxygen Isotope Fractionation between Synthetic Aragonite and Water: Influence of Temperature and Mg2+ Concentration." *Geochimica et Cosmochimica Acta* 71 (19): 4704–15. doi:10.1016/j.gca.2007.04.019.

Larson, Robert P, James M Byrne, Daniel L Johnson, Matthew G Letts, and Stefan W Kienzle. 2011. "Modelling Climate Change Impacts on Spring Runoff for the Rocky Mountains of Montana and Alberta I: Model Development, Calibration and Historical Analysis RID F-9528-2010." *Canadian Water Resources Journal* 36 (1): 17–33. doi:10.4296/cwrj3601017.

Leonard, Eric M, and M a Reasoner. 1999. "A Continuous Holocene Glacial Record Inferred from Proglacial Lake Sediments in Banff National Park, Alberta, Canada." *Quaternary Research* 51 (1): 1–13. doi:10.1006/qres.1998.2009.

Li, H. C., and T. L. Ku. 1997. "Δ13C-Δ18O Covariance as a Paleohydrological Indicator for Closed-Basin Lakes." *Palaeogeography, Palaeoclimatology, Palaeoecology* 133 (1–2): 69–80. doi:10.1016/S0031-0182(96)00153-8.

Licciardi, Joseph M., Peter U. Clark, Edward J. Brook, David Elmore, and Pankaj

Sharma. 2004. “Variable Responses of Western U.S. Glaciers during the Last Deglaciation.” *Geology* 32 (1): 81–84. doi:10.1130/G19868.1.

Liu, Zhongfang, Kei Yoshimura, Gabriel J. Bowen, Nikolaus H. Buenning, Camille Risi, Jeffrey M. Welker, and Fasong Yuan. 2014. “Paired Oxygen Isotope Records Reveal Modern North American Atmospheric Dynamics during the Holocene.” *Nature Communications* 5. Nature Publishing Group: 1–7. doi:10.1038/ncomms4701.

Luckman, B. H. 2000. “The Little Ice Age in the Canadian Rockies.” *Geomorphology* 32 (3–4): 357–84. doi:10.1016/S0169-555X(99)00104-X.

Luckman, Brian H. 1994. “Evidence for Climatic Conditions Between CA. 900-1300 A.D. in the Southern Canadian Rockies.” In *The Medieval Warm Period*, 171–82. doi:10.1007/978-94-011-1186-7.

MacDonald, G.M. 1989. “Postglacial Paleoecology of the Sub-Alpine Forest-Grassland Ecotone: New Insights on Vegetation and Climate Change in the Canadian Rocky Mountains and Adjacent Foothills.” *Paleogeography, Paleoclimatology, Paleoecology* 75: 155–73.

MacDonald, Glen M. 1982. “Late Quaternary Paleoenvironments of the Morley Flats and Kananaskis Valley of Southwestern Alberta.” *Canadian Journal of Earth Sciences* 19 (1): 23–35. doi:10.1139/e82-003.

Mann, Michael E. 2008. “Smoothing of Climate Time Series Revisited.” *Geophysical Research Letters* 35 (16): 1–5. doi:10.1029/2008GL034716.

Mantua, Nathan J, and Steven R Hare. 2002. “The Pacific Decadal Oscillation.” *Journal of Oceanography* 58 (1991): 35–44.

Marshall, Shawn J., Eric C. White, Michael N. Demuth, Tobias Bolch, Roger Wheate, Brian Menounos, Matthew J. Beedle, and Joseph M. Shea. 2011. “Glacier Water Resources on the Eastern Slopes of the Canadian Rocky Mountains.” *Canadian Water Resources Journal* 36 (2): 109–34. doi:10.4296/cwrj3602823.

Menounos, Brian, Gerald Osborn, John J. Clague, and Brian H. Luckman. 2009. “Latest Pleistocene and Holocene Glacier Fluctuations in Western Canada.” *Quaternary Science Reviews* 28 (21–22). Elsevier Ltd: 2049–74. doi:10.1016/j.quascirev.2008.10.018.

Newman, Matthew, Gilbert P. Compo, and Michael A. Alexander. 2003. “Letters of the Pacific Decadal Oscillation.” *Journal of Climate* 16 (23): 3853–57.

Osborn, Gerald, and Lisa Gerloff. 1997. “Latest Pleistocene and Early Holocene Fluctuations of Glaciers in the Canadian and Northern American Rockies.” *Quaternary International* 6182 (96): 7–19. doi:10.1016/S1040-6182(96)00026-2.

Parnell, A. C., J. Haslett, J. R M Allen, C. E. Buck, and B. Huntley. 2008. “A Flexible Approach to Assessing Synchroneity of Past Events Using Bayesian Reconstructions of Sedimentation History.” *Quaternary Science Reviews* 27 (19–20): 1872–85. doi:10.1016/j.quascirev.2008.07.009.

Parnell, Andrew C., Caitlin E. Buck, and Thinh K. Doan. 2011. “A Review of Statistical

Chronology Models for High-Resolution, Proxy-Based Holocene Palaeoenvironmental Reconstruction." *Quaternary Science Reviews* 30 (21–22): 2948–60. doi:10.1016/j.quascirev.2011.07.024.

Rasmussen, J B, and D J Rowan. 1997. "Wave Velocity Thresholds for Fine Sediment Accumulation in Lakes, and Their Effect on Zoobenthic Biomass and Composition." *Journal Of the North American Benthological Society* 16 (3): 449–65. doi:10.2307/1468137.

Reasoner, M. A., G. Osborn, and N. W. Rutter. 1994. "Age of the Crowfoot Advance in the Canadian Rocky Mountains: A Glacial Event Coeval with the Younger Dryas Oscillation." *Geology* 22 (5): 439–42. doi:10.1130/0091-7613(1994)022<0439:AOTCAI>2.3.CO;2.

Reimer, Paula J, Edouard Bard, Alex Bayliss, J Warren Beck, Paul G Blackwell, Christopher Bronk Ramsey, Caitlin E Buck, et al. 2013. "IntCal13 and Marine13 Radiocarbon Age Calibration Curves 0–50,000 Years Cal BP." *Radiocarbon* 55 (04). Cambridge University Press: 1869–87. doi:10.2458/azu_js_rc.55.16947.

Rodionov, S. N., N. A. Bond, and J. E. Overland. 2007. "The Aleutian Low, Storm Tracks, and Winter Climate Variability in the Bering Sea." *Deep-Sea Research Part II: Topical Studies in Oceanography* 54 (23–26): 2560–77. doi:10.1016/j.dsr2.2007.08.002.

Rowan, DJ, J Kalff, and JB Rasmussen. 1992. "Estimating the Mud Deposition Boundary Depth in Lakes from Wave Theory." *Canadian Journal of Fisheries and Aquatic Sciences* 49: 2489.

Rozanski, Kazimierz, Luis Araguás-Araguás, and Roberto Gonfiantini. 1992. "Relation Between Long-Term Trends of Oxygen-18 Isotope Composition of Precipitation And." *Science* 258 (5084): 981–85. http://www.jstor.org/stable/2881675%0Ahttp://links.jstor.org/action/showPublisher?publisherCode=aaas.

Sauchyn, David J., Stroich, Jenifer., Beriault, Antonie. 2003. "A Paleoclimatic Context for the Drought of 1999-2001 in the Northern Great Plains of North America." *The Geographical Journal* 169 (2): 158–67. doi:10.1111/1475-4959.05003.

Sauchyn, D. J., D. M. Cruden, and X. Q. Hu. 1998. "Structural Control of the Morphometry of Open Rock Basins, Kananaskis Region, Canadian Rocky Mountains." *Geomorphology* 22 (3–4): 313–24. doi:10.1016/S0169-555X(97)00083-4.

Sauchyn, David J., Jeannine-Marie St-Jacques, and Brian H. Luckman. 2015. "Long-Term Reliability of the Athabasca River (Alberta, Canada) as the Water Source for Oil Sands Mining." *Proceedings of the National Academy of Sciences* 112 (41): 12621–26. doi:10.1073/pnas.1509726112.

Sauchyn, David, Jessica Vanstone, Jeannine Marie St Jacques, and Robert Sauchyn. 2015. "Dendrohydrology in Canada's Western Interior and Applications to Water Resource Management." *Journal of Hydrology* 529 (P2). Elsevier B.V.: 548–58. doi:10.1016/j.jhydrol.2014.11.049.

Shapley, M.D., E. Ito, and J.J. Donovan. 2009. “Lateglacial and Holocene Hydroclimate Inferred from a Groundwater Flow-through Lake, Northern Rocky Mountains, USA.” *The Holocene* 19 (4): 523–35. doi:10.1177/0959683609104029.

Shuman, Bryan N., Cody Routson, Nicholas McKay, Sherilyn Fritz, Darrell Kaufman, Matthew E. Kirby, Connor Nolan, Gregory T. Pederson, and Jeannine Marie St-Jacques. 2018. “Placing the Common Era in a Holocene Context: Millennial to Centennial Patterns and Trends in the Hydroclimate of North America over the Past 2000 Years.” *Climate of the Past* 14 (5): 665–86. doi:10.5194/cp-14-665-2018.

Smith, Daniel J, Daniel P. Mccarthy, and Margaret E Colenutt. 1995. “Little Ice Age Glacial Activity in Peter Lougheed and Elk Lakes Provincial Parks, Canadian Rocky Mountains.” *Canadian Journal of Earth Sciences* 32 (5): 579–89. doi:10.1139/e95-049.

Stansell, Nathan D., Byron A. Steinman, Mark B. Abbott, Michael Rubinov, and Manuel Roman-Lacayo. 2013. “Lacustrine Stable Isotope Record of Precipitation Changes in Nicaragua during the Little Ice Age and Medieval Climate Anomaly.” *Geology* 41 (2): 151–54. doi:10.1130/G33736.1.

Steinman, Byron A., Daniel B. Nelson, Mark B. Abbott, Nathan D. Stansell, Matthew S. Finkenbinder, and Bruce P. Finney. 2019. “Lake Sediment Records of Holocene Hydroclimate and Impacts of the Mount Mazama Eruption, North-Central Washington, USA.” *Quaternary Science Reviews* 204: 17–36.

Steinman, Byron A., David P. Pompeani, Mark B. Abbott, Joseph D. Ortiz, Nathan D. Stansell, Matthew S. Finkenbinder, Lorita N. Mihindukulasooriya, and Aubrey L. Hillman. 2016. “Oxygen Isotope Records of Holocene Climate Variability in the Pacific Northwest.” *Quaternary Science Reviews* 142. Elsevier Ltd: 40–60. doi:10.1016/j.quascirev.2016.04.012.

Steinman, Byron A., Michael F. Rosenmeier, Mark B. Abbott, and Daniel J. Bain. 2010. “The Isotopic and Hydrologic Response of Small, Closed-Basin Lakes to Climate Forcing from Perspective Models: Application to Paleoclimate Studies in Upper Columbia River Basin.” *Limnology and Oceanography* 55 (6): 2231–45. doi:10.4319/lo.2010.55.6.2231.

Stuiver, Minze, and Paula Reimer. 1993. “EXTENDED 14C DATA BASE AND REVISED CALIB 3.014C AGE CALIBRATION PROGRAM.” *Radiocarbon* 35 (1): 215–30. doi:10.1017/S0033822200013862.

Sung, Mi Kyung, Soon Il An, Baek Min Kim, and Sung Ho Woo. 2014. “A Physical Mechanism of the Precipitation Dipole in the Western United States Based on PDO-Storm Track Relationship.” *Geophysical Research Letters* 41 (13): 4719–26. doi:10.1002/2014GL060711.

Swanson, R H, D L Golding, R L Rothwell, and P Y Bernier. 1986. “Hydrologic Effects of Clear-Cutting at Marmot Creek and Streeter Watersheds, Alberta.” *Information Report Northern Forestry Centre, Canadian Forestry Service* NOR-X-278.

Thompson, J.B., S. Schultze-Lam, T.J. Beveridge, and D.J. Des Marais. 1997. “Whiting Events: Biogenic Origin Due to the Photosynthetic Activity of Cyanobacterial

Picoplankton." *Limnology and Oceanography* 42 (1): 133–41. doi:10.4319/lo.1997.42.1.0133.

Whitlock, Cathy, Walter E. Dean, Sherilyn C. Fritz, Lora R. Stevens, Jeffery R. Stone, Mitchell J. Power, Joseph R. Rosenbaum, Kenneth L. Pierce, and Brandi B. Bracht-Flyr. 2012. "Holocene Seasonal Variability Inferred from Multiple Proxy Records from Crevice Lake, Yellowstone National Park, USA." *Palaeogeography, Palaeoclimatology, Palaeoecology* 331–332. Elsevier B.V.: 90–103. doi:10.1016/j.palaeo.2012.03.001.

Williams, John W., Bryan Shuman, Patrick J. Bartlein, Noah S. Diffenbaugh, and Thompson Webb. 2010. "Rapid, Time-Transgressive, and Variable Responses to Early Holocene Midcontinental Drying in North America." *Geology* 38 (2): 135–38. doi:10.1130/G30413.1.

Yu, Bin, and FW Zwiers. 2007. "The Impact of Combined ENSO and PDO on the PNA Climate : A 1 , 000-Year Climate Modeling Study The Impact of Combined ENSO and PDO on the PNA Climate : A 1 , 000-Year Climate Modeling Study." *Climate Dynamics* 29: 837–51. doi:10.1007/s00382-007-0267-4.

Zdanowicz, C. M., G. A. Zielinski, and M. S. Germani. 1999. "Mount Mazama Eruption: Calendrical Age Verified and Atmospheric Impact Assessed." *Geology* 27 (7): 621–24. doi:10.1130/0091-7613(1999)027<0621:MMECAV>2.3.CO.

Zhao, Cheng, Zicheng Yu, Emi Ito, and Yan Zhao. 2010. "Holocene Climate Trend , Variability , and Shift Documented by Lacustrine Stable-Isotope Record in the Northeastern United States." *Quaternary Science Reviews* 29 (15–16). Elsevier Ltd: 1831–43. doi:10.1016/j.quascirev.2010.03.018.